TECHNICAL MEMORANDUM
X-192

WIND-TUNNEL INVESTIGATION AT HIGH SUBSONIC SPEEDS TO DETERMINE STABILITY AND CONTROL CHARACTERISTICS OF ANTITANK MISSILES WITH RAM-PRESSURE JET CONTROLS ON A RING TAIL

By Raymond D. Vogler

Langley Research Center
Langley Field, Va.

NATIONAL AERONAUTICS AND SPACE ADMINISTRATION
WASHINGTON
February 1960

[redacted]

NATIONAL AERONAUTICS AND SPACE ADMINISTRATION

TECHNICAL MEMORANDUM X-192

WIND-TUNNEL INVESTIGATION AT HIGH SUBSONIC SPEEDS TO DETERMINE STABILITY AND CONTROL CHARACTERISTICS OF ANTITANK MISSILES WITH RAM-PRESSURE JET CONTROLS ON A RING TAIL*

By Raymond D. Vogler

SUMMARY

A wind-tunnel investigation was made at high subsonic speeds in the Langley high-speed 7- by 10-foot tunnel to determine the stability characteristics and the effectiveness of ram-pressure jet controls on three models of antitank missiles with ring tails. Tail size and position, body shape, ram-pressure ducts of various sizes, duct inlet positions, and slot exit areas were some of the factors involved in the investigation. The longitudinal stability and drag of the models were strongly influenced by interference between combinations of these geometric factors at different Mach numbers. Smaller ducts in the ring tail generally had more desirable drag and stability characteristics than larger ones, and ducts collecting air from inside the ring tail were more destabilizing than ducts collecting air from outside the ring tail. With the rear of the body faired to a boattail shape, a configuration with ducts collecting air from outside the ring tail was obtained that had stability and control through the Mach number and angle-of-attack range investigated.

Author

INTRODUCTION

High-subsonic-speed tests of a ground-to-ground antitank missile were made in the Langley high-speed 7- by 10-foot tunnel. The missile is tube launched, rocket-sustained in flight, and electronically guided. The primary purpose of these tests was to determine a stable configuration from different bodies, tail sizes, and tail positions. In addition, tests were made to determine the effectiveness of ram-pressure jet and spoiler controls in producing pitching and yawing moments.

*Title, Unclassified.

[redacted]

COEFFICIENTS AND SYMBOLS

The wind and body axes to which the coefficients are referred are given in figure 1.

C_L	lift coefficient, $\frac{\text{Lift}}{qA}$
C_N	normal-force coefficient, $\frac{\text{Normal force}}{qA}$
C_D	drag coefficient, $\frac{\text{Drag}}{qA}$
C_A	axial-force coefficient, $\frac{\text{Axial force}}{qA}$
C_m	pitching-moment coefficient, $\frac{\text{Pitching moment}}{qAd}$
C_n	yawing-moment coefficient, $\frac{\text{Yawing moment}}{qAd}$
q	tunnel dynamic pressure, $\rho V^2/2$, lb/sq ft
ρ	mass density of air, slugs/cu ft
V	free-stream velocity, ft/sec
A	reference area, $\pi d^2/4$
d	maximum body diameter
M	Mach number
α	angle of attack, deg
$\frac{dC_m}{dC_L}$	slope of pitching-moment curve at $\alpha = 0^\circ$
X,Z	body reference axes
X_w,Z_w	wind reference axes

[redacted]

APPARATUS AND MODEL

The models were mounted on a sting support in the Langley high-speed 7- by 10-foot tunnel. A strain-gage balance attached to the end of the sting and contained within the model was used to measure the forces and moments.

Three all-metal models were tested. Model 1 (fig. 2(a)) was composed of an ogive nose piece, a short cylindrical body, a parabolic afterbody, and a ring tail attached to the afterbody with flat-plate supporting fins set vertically and horizontally into the afterbody and parallel to the model axis. Between each of the four pairs of fins there could be inserted a duct plate which with the fins, ring tail, and backplate formed four ducts which directed free-stream air to holes or slots in the trailing edge of the ring tail and duct plate (fig. 2(b)). The use of holes and slots was to determine the relative effectiveness of the two types of exits. By virtue of the ram pressure at the duct inlet, air was forced outward through holes in the ring tail or inward toward the model central axis through holes in the duct plate. This duct system with suitable seals or valves formed a jet control for the model. The jets were operated as pairs, one on either side of the tail, to produce pitching and yawing moments. Model 1 had tails with chords of 2.5 and 3.5 inches and the longitudinal position of the tail could be varied within small limits. In one test the ogive nose of the model was replaced with a 2-inch-diameter cylinder with hemispherical nose.

Model 2 (fig. 3) was composed of the nose piece of model 1, a long cylindrical body, a truncated ogive afterbody, and an attached ring tail. There were two tail rings, one of 6-inch and one of 7-inch diameter, with a common width of 4 inches. The method of attachment and duct construction were similar to those of model 1, but model 2 had no holes or slots for jet controls. Since the tails were larger in diameter than the body, guide feet were attached to the front of the cylindrical part of the body, the purpose of the feet being to aline the model in its launching tube.

Model 3 (fig. 4(a)) had a body similar to model 2 but was longer and had a cone-plus-cylinder afterbody shape. The ring tail was attached to the afterbody with four fins which split the ducts at their trailing edges. Fairings over the control actuator mechanisms of the flying missile were simulated by an increased thickness of the fins at the rear of the ducts. The details of the ducts, designated "inside" and "outside," are given in figure 4(b). The entrance to the inside duct was inside the ring tail and the entrance to the outside duct was outside the ring tail. The outside entrance was made by cutting a trapezoidal notch in the tail and extending the duct plate to the leading edge of the ring tail. The inside ducts were untapered in depth from front to rear. Outside ducts were tapered and untapered. Jet holes or slots were in both the ring tail and

the duct plate, similar to those in model 1 (fig. 2(b)). The width of the slot in the ring tail could be adjusted by means of the backplate which blocked the duct at the rear. The duct plates were removable for changing slot widths in them. The spoilers (fig. 4(b)) were thin flat plates and were mounted in a special slot at the tail trailing edge. This model also had guide feet and small antennas (fig. 4(a)) that could be mounted on the rear inside surface of the ring tail or on the rear of the afterbody. The soft wood fairing (fig. 4(a)) on the afterbody was shaped by hand to eliminate sharp breaks on the original afterbody.

Models 2 and 3 were full scale and model 1 was 0.86 full scale.

L
6
2
2

TESTS AND CORRECTIONS

Data were obtained from tests of three models in the Langley high-speed 7- by 10-foot tunnel at angles of attack from -10° to 10°. Model 1 was tested with ring tails in three longitudinal positions and with tails of two widths. Inside ducts only were tested on this model and the jet exits were not variable in area. Model 2 was tested without controls. Tail diameter, tail position, and different shaped guide feet were investigated. Model 3 was tested with inside and outside ducts of different shapes and jet exits that could be varied, but with a fixed tail position, diameter, and width. Spoilers of two shapes and two projections were tested on this model.

The Mach number range was from 0.75 to 0.90 and the corresponding Reynolds number based on a body diameter of 0.43 foot varied from 1.63×10^6 to 1.784×10^6.

The only corrections applied to the data were blocking corrections to the Mach number and dynamic pressure as determined by the method of reference 1.

RESULTS AND DISCUSSION

Model 1.- The aerodynamic characteristics of model 1 obtained with the jet controls operating and not operating are presented in figure 5. It is readily seen that the controls are effective but the model is unstable. The overall slopes of the pitching-moment curves indicate that the aerodynamic center of the model is ahead of the moment center by approximately 0.6d to 0.7d, depending upon Mach number. The data indicate that blowing outward from the holes is more effective than blowing outward from the slot. Since the total exit area of the holes was less than the exit area of the slot, this might result in a greater

buildup of ram pressure in the duct with hole exits and a greater penetration of the jets into the free stream. A combination of inward and outward blowing is 25 to 30 percent more effective than outward blowing alone. With all four outside jets blowing - a possible controls-neutral condition - the stability characteristics are the same as for all jets closed, but the blowing jets increase the drag of the model by 15 to 20 percent.

In order to determine some of the causes of the model instability and develop some possible improvements, some tests of the body alone and of the model with different ring-tail locations were made. The data of these tests are presented in figures 6 to 8, and some of the results are summarized in figure 9. This figure shows that for similar configurations the 2.5-inch-wide (higher aspect ratio) tail band is not as unstable as the 3.5-inch-wide tail. Some of this decrease in instability may be attributed to an increase in tail length of about 0.5 inch since the 2.5-inch-wide tail was made by removing 1 inch at the leading edge of the 3.5-inch-wide tail. However, the change in instability is never less than would be effected by an equivalent 0.5-inch increase in tail length and is generally comparable to that obtained by an increase in tail length of 1 to 4 inches. As the 2.5-inch-wide tail alone (ducts off) is moved rearward by 1-inch increments, the instability of the model decreases approximately as expected as a result of the increased tail length, except with the tail in the rear position at $M = 0.9$. Here the model becomes very stable at zero angle of attack but reverts to its unstable condition at higher angles of attack (fig. 6(c)).

Adding the ducts to either ring tail of model 1 considerably increases the instability (fig. 9). Blowing from the four outside jet exits had little effect on the stability of the model with the 3.5-inch tail (figs. 5 and 9), but, with the 2.5-inch tail, the instability was changed to almost neutral stability through the Mach range at low angles of attack (figs. 6 and 9). As expected, the drag of the model with the 3.5-inch tail was slightly more than with the 2.5-inch tail with ducts on and no blowing jets; but, blowing from the four outside jet exits increased the model drag by 40 to 50 percent with the 2.5-inch tail as compared with 15 to 20 percent with the 3.5-inch tail (figs. 5 and 6). With ducts off the 2.5-inch tail gave less drag in the midposition than in the forward or rear positions. Figures 7 and 8 show the effect on stability and drag of adding the supporting fins and the ring tail to the body. The effects of modifying the nose of model 1 and the body-alone characteristics of model 2 are also shown in figure 8.

Model 2.- Model 2 (fig. 3) is another preliminary design of an antitank missile. This model differed from model 1 in having more of its body cylindrical and having ring tails larger in diameter than the body itself. Feet added to position the model in the launching tube made the overall diameter equal to the tail diameter. The rectangular

feet were destabilizing, but the circular feet were not too objectionable (figs. 10 and 11). No controls were tested on this model, the object simply being to determine stability characteristics of basic configurations with different tail sizes and positions. These characteristics are shown in figures 10 and 11, and the results are summarized in figure 12. In the rearward position, the 7-inch-diameter tail is very stable and the 6-inch-diameter tail is generally about neutrally stable, through the angle-of-attack and Mach number range. In the forward position the 6-inch tail is very unstable while the 7-inch tail is stable only at the higher angles of attack, except at $M = 0.9$ where it is stable through the angle-of-attack range. The drag of the model with the 7-inch tail in the unstable (forward) position is more than the drag of the stable configuration. This increased drag with the tail in the forward position is probably due to flow separation resulting from too rapid area expansion in the flow passage between the afterbody and tail. The 6-inch tail does not have as large variations in drag with tail position as the 7-inch tail, but there are much larger variations in lift with tail positions at a given angle of attack with the 6-inch tail than with the 7-inch tail.

L 6 2 2

Model 3.- In the design of model 3 (fig. 4) some of the test results from models 1 and 2 were taken into consideration. Since installation of the ducts on model 1 made the model more unstable, it was believed that this instability could be reduced by reducing the blockage of the ducts and the flow disturbance at the leading edge of the tail. This modification was made by changing the shape of the afterbody, moving the duct entrances farther back on the tail, using shorter ducts inside the tail ring, or by cutting notches in the tail ring forming the distinguishing feature of what is referred to as outside ducts. Since the flying missile would require guide feet for proper positioning in the launching tube and receiving antennas for guidance control, both were tested in two positions. Figure 13 shows that changing the position of either did not have a great effect on model stability. In all remaining tests (figs. 14 to 18) the feet were in the rear position and the antennas were attached to the rear of the afterbody.

Two spoilers differing in plan form were attached to the trailing edge of the tail and were tested simultaneously as possible pitch and yaw control devices. In this case and in some of the jet-control configurations the model is not symmetrical in pitch and yaw and the data for both moments are presented along with the normal and axial-force data, for an angle-of-attack range. The spoiler projected equally at both ends yielded increments of moment (C_n, fig. 14) about proportional to the spoiler frontal area, but the spoiler projected unequally at the ends showed decreasing effectiveness (C_m, fig. 14) with increasing projection. However, the latter spoiler was more effective than the former based on moment increment per unit of frontal area of the projected spoiler (fig. 14).

The results obtained with jet controls used in conjunction with the small inside ducts are shown in figure 15. In this case the control power of the jets is again good, but the instability of the model is generally about the same as with controls and ducts off. A faired afterbody (fig. 4(a)), similar to the afterbody of model 2, improved the stability at small negative angles of attack and reduced the drag to about that of the model with ducts and jets off, without impairing the control power of the jets.

The yawing-moment coefficients presented may also be considered as pitching-moment coefficients at zero angle of attack through a sideslip range, in which case the average incremental pitching-moment coefficients through the Mach range at zero angle of attack for the 0.062-, 0.125-, and 0.187-inch-slot jets are approximately 0.230, 0.420, and 0.490, respectively. These values give some indication of the effect of jet-exit-slot width on incremental moments.

Moving the ring tail rearward 0.6 inch on this model (fig. 16) produced a stabilizing influence that was four or five times greater than expected from the increase in tail length. This change gave a model configuration that was generally stable or neutrally stable except near $\alpha = 0^\circ$ at $M = 0.9$ and is indicative of the sensitivity of tail effectiveness to tail position. However, with the large inside ducts installed and controls operating, the model became as unstable as it was with the tail in the original position with small ducts on and controls operating. The large ducts on the tail in the more rearward position did give about 60 percent more pitching moment than the small ducts on the tail in the forward position for the same slot width, at $\alpha = 0^\circ$.

The characteristics of the model with outside ducts on the ring tail are presented in figure 17 and summarized in figure 18. It will be noticed that the pitching-moment curves show small irregularities in slope at lower lift coefficients and then very definite changes in slope at higher lift coefficients. These small irregularities in linearity may result from flow separation which is not stabilized at any particular point on the afterbody until a sizable angle of attack is reached. The afterbody fairing eliminated some of the nonlinearity of the pitching-moment curves and extended the stable range of the model to higher angles of attack. Throughout this series of tests with outside ducts, the control exits on the sides were eight 0.125-inch-diameter holes. The exits for top and bottom controls were adjustable slots. Sufficient testing time was not available to permit determining the relative effectiveness of hole and slot exits on this model. Difficulty in setting slot widths at a predetermined value accounts for the fact that the upper and lower slots are not the same width. The values of dC_m/dC_L shown in figure 18 were obtained at $\alpha = 0^\circ$. However, one might be justified in measuring the overall slopes between about $\pm 4^\circ$, in which case the stability would generally be greater than indicated by the curves of figure 18 and would

vary less with Mach number. The data as shown indicate that the model with the small untapered ducts with faired afterbody is a stable configuration. The small tapered ducts give neutral stability, and adding the afterbody fairing gives some increase in stability. Tapering the small duct increases the power of the control and reduces the drag. Increasing the size (frontal depth) of the tapered duct increases the control power, the drag, and the stability at low Mach numbers but severely decreases the stability at M = 0.90. Doubling the slot width on this duct approximately doubled the pitching moment.

CONCLUSIONS

A wind-tunnel investigation was made at high subsonic speeds to determine the stability characteristics and the effectiveness of jet controls on three models of antitank missiles with ring tails. Tail size and position, body shape, ram-pressure ducts of various sizes, duct-inlet position, and slot-exit areas were variable factors in the investigation. From the data obtained the following conclusions are reached:

1. The longitudinal stability and the drag of the models were not dependent solely on geometric factors such as tail size and position, duct size, and body shape, but were also dependent upon interference effects between combinations of these geometric factors at different Mach numbers.

2. Ducts collecting air from inside the ring tail were more destabilizing than ducts collecting air from outside the ring tail, and with either type of duct a boattail shape of the rear of the missile body gave better stability characteristics than other shapes.

3. The smaller ducts generally had more desirable drag and stability characteristics than the larger, and a model configuration with ducts collecting air from outside the ring tail was obtained that had stability and control through the Mach number and angle-of-attack range investigated.

Langley Research Center,
National Aeronautics and Space Administration,
Langley Field, Va., August 26, 1959.

REFERENCE

1. Herriot, John G.: Blockage Corrections for Three-Dimensional-Flow Closed-Throat Wind Tunnels, With Consideration of the Effect of Compressibility. NACA Rep. 995, 1950. (Supersedes NACA RM A7B28.)

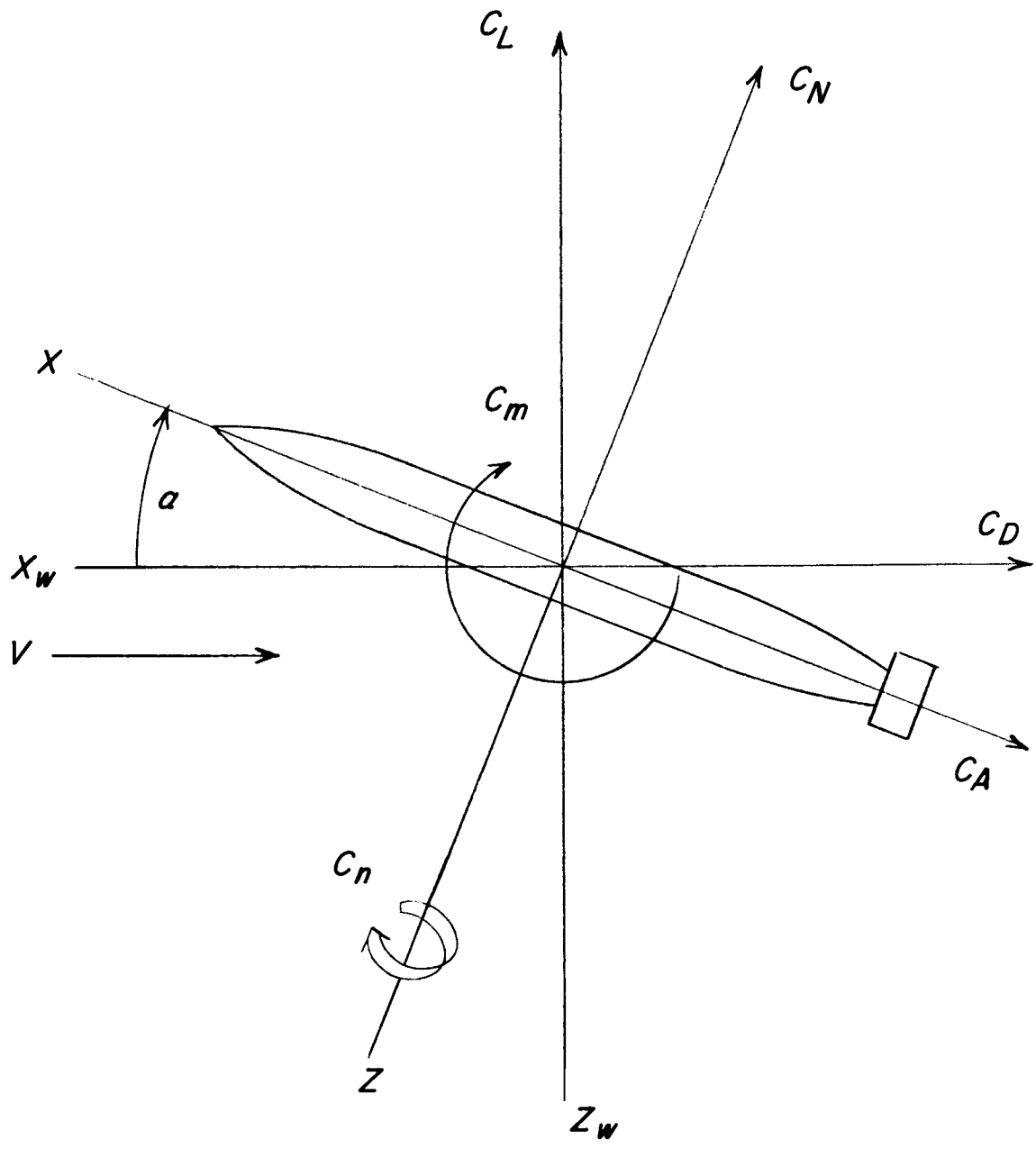

Figure 1.- Wind and body axes. Positive values indicated by arrows.

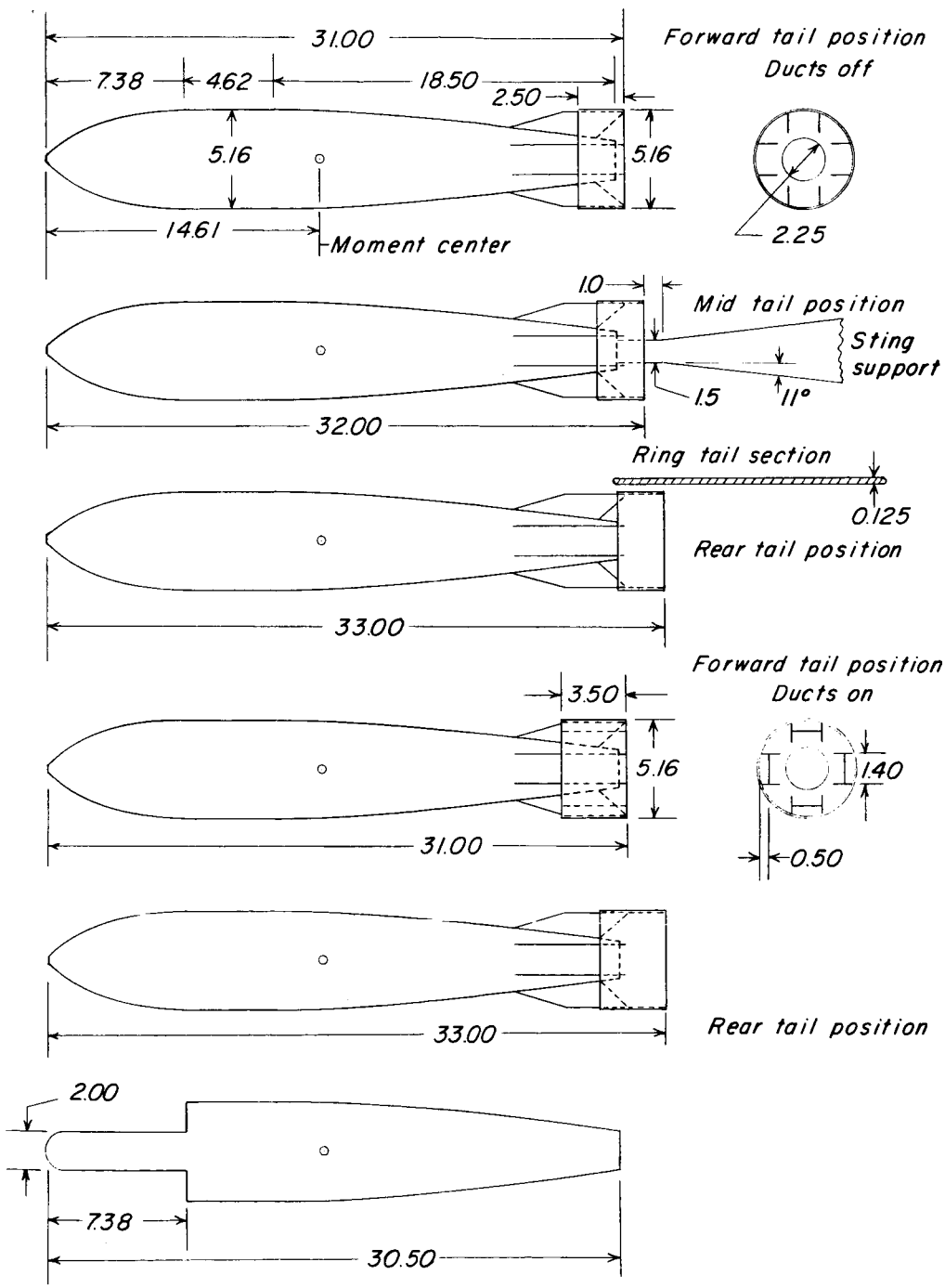

(a) Geometric characteristics and tail arrangements.

Figure 2.- Model 1. Dimensions in inches.

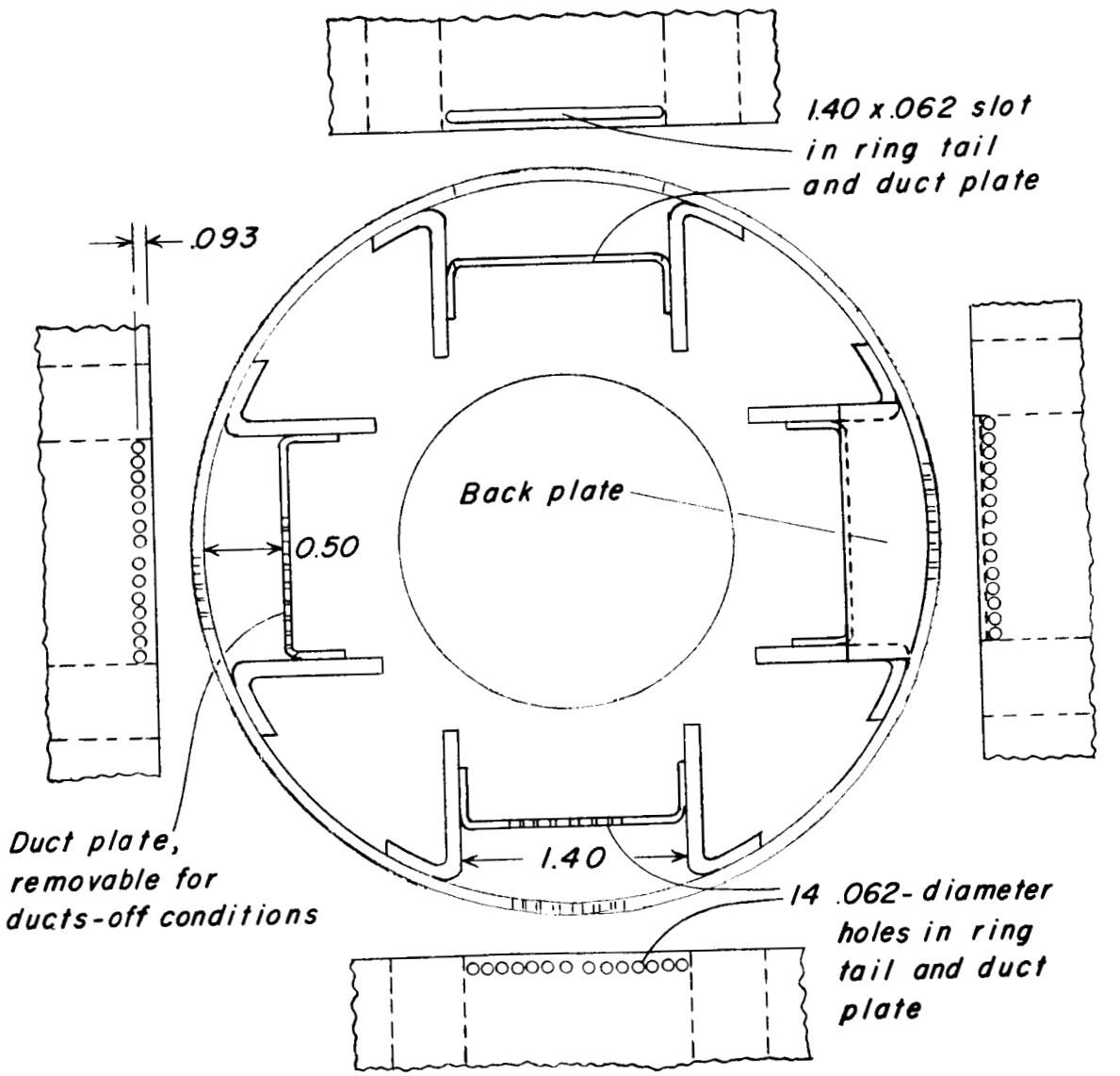

(b) Details of jet control.

Figure 2.- Concluded.

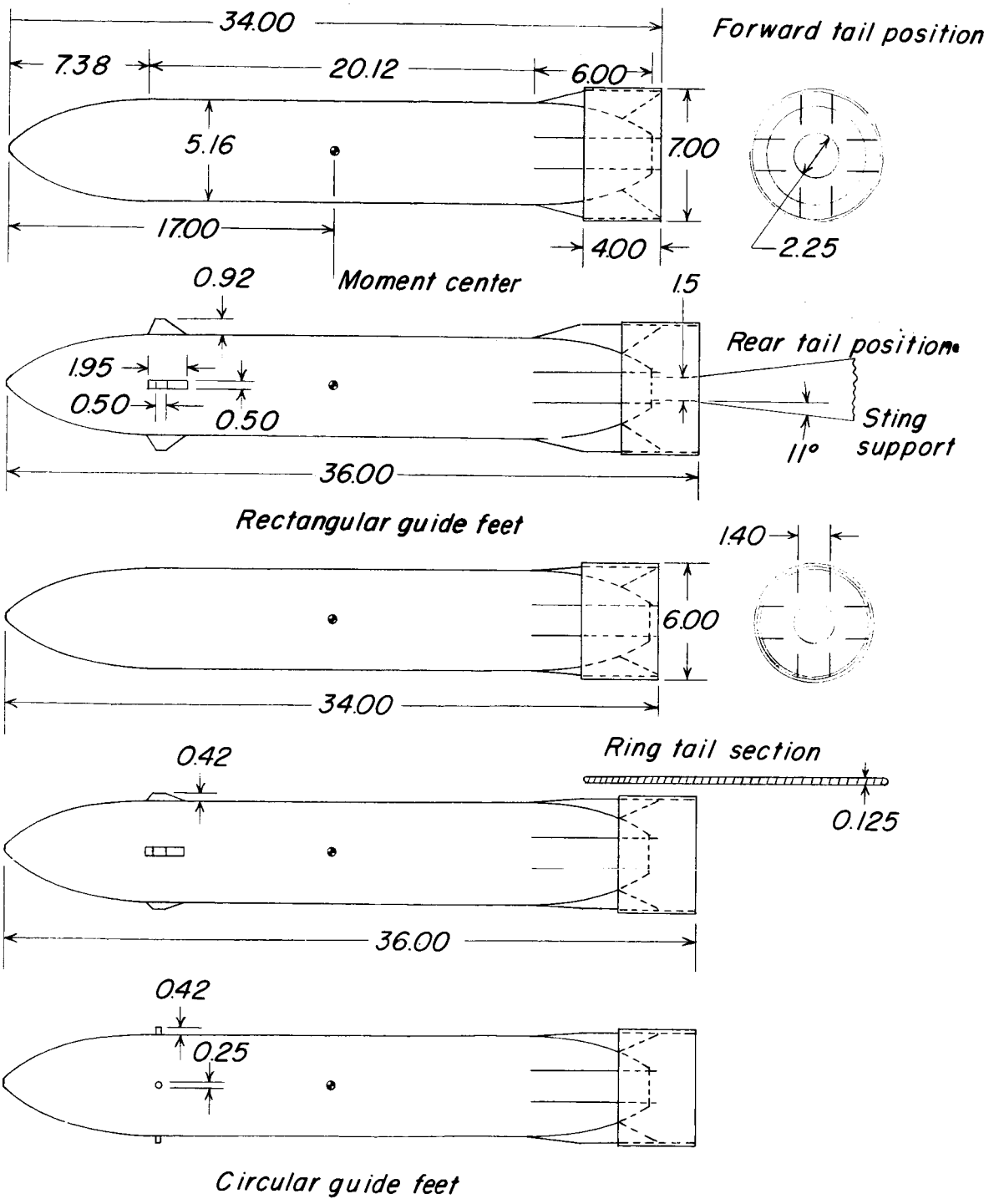

Figure 3.- Geometric characteristics and tail arrangements of model 2. Dimensions in inches.

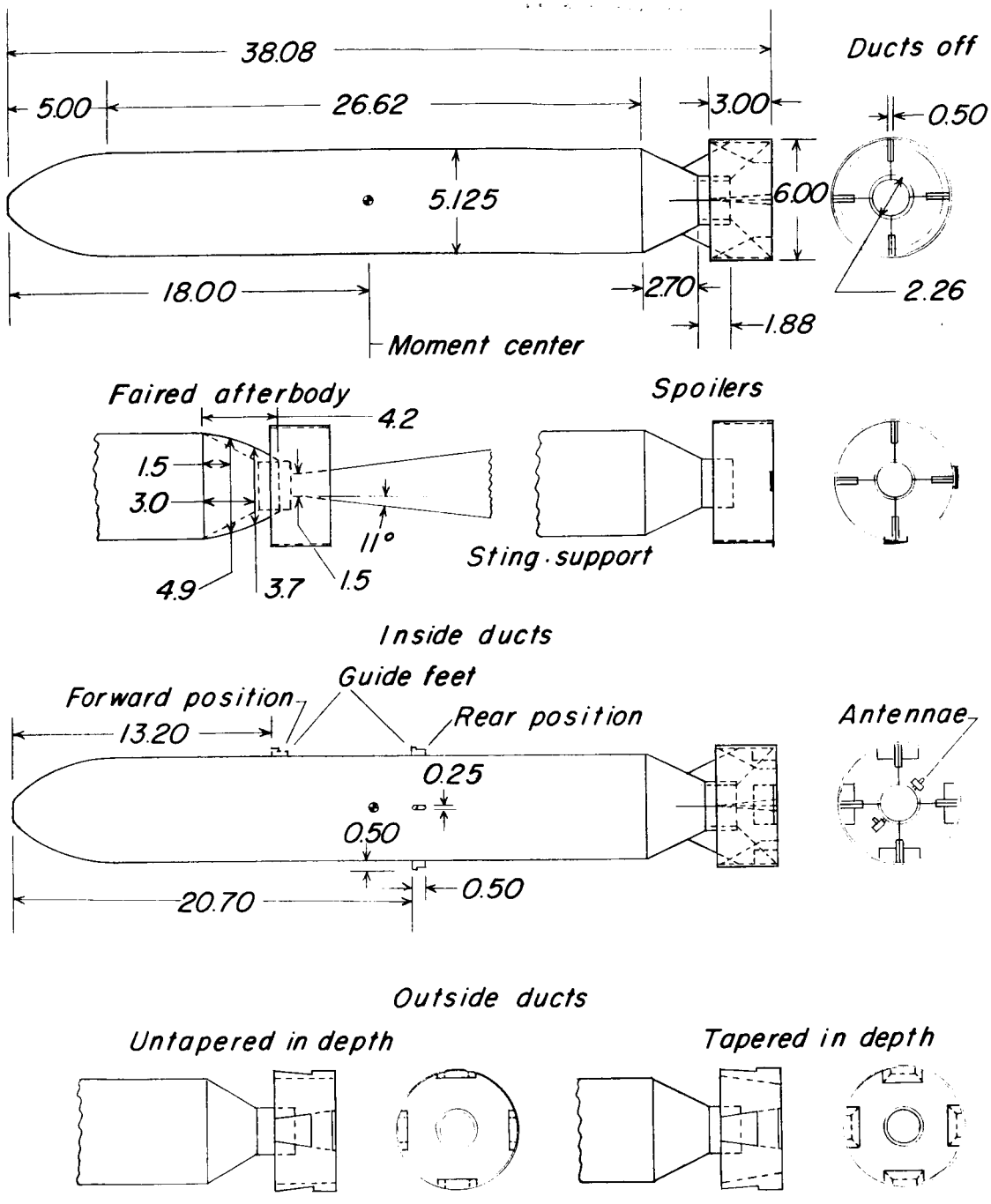

(a) Geometric characteristics and duct arrangements.

Figure 4.- Model 3. Dimensions in inches.

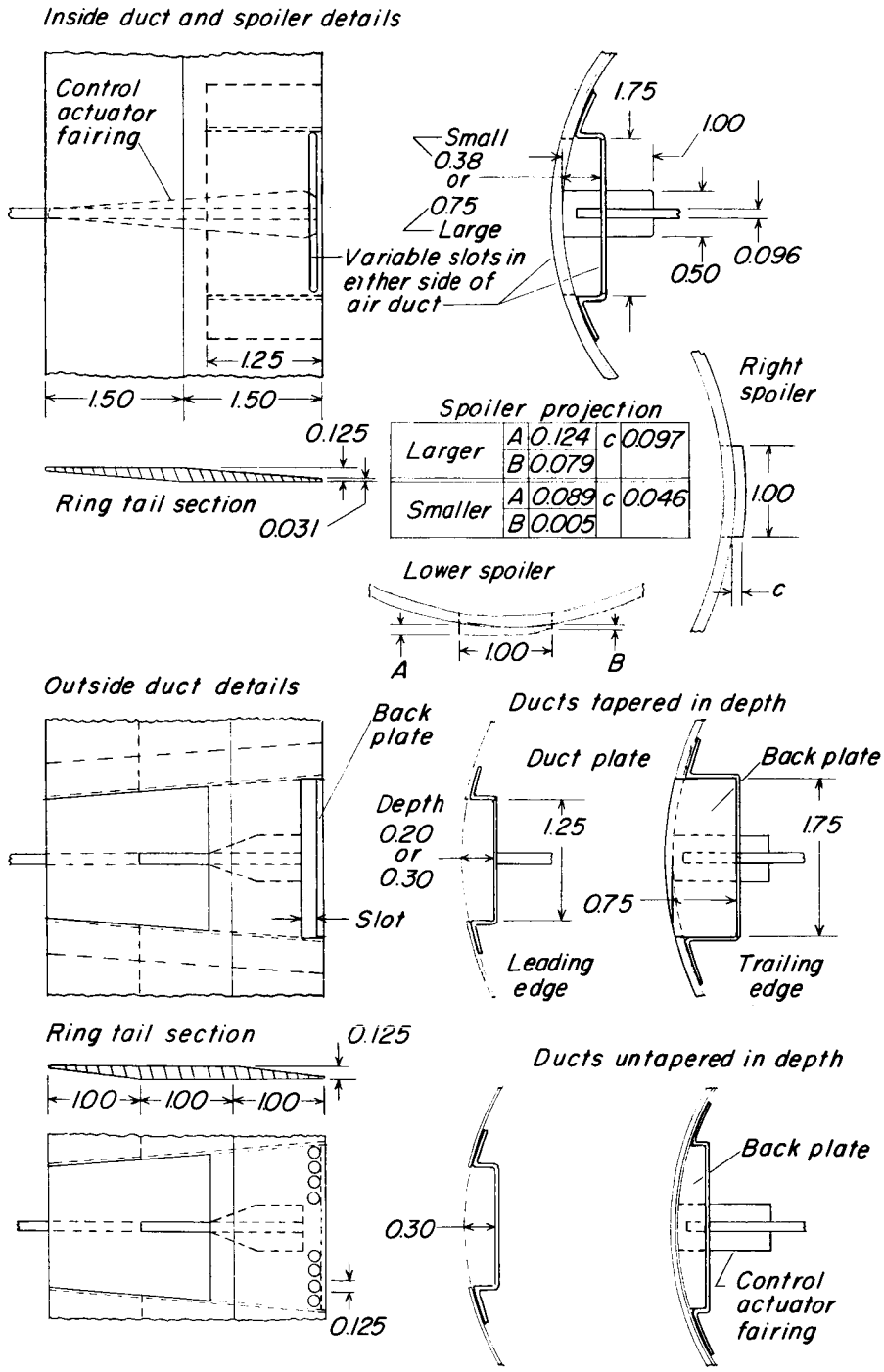

(b) Details of various controls.

Figure 4.- Concluded.

L-622

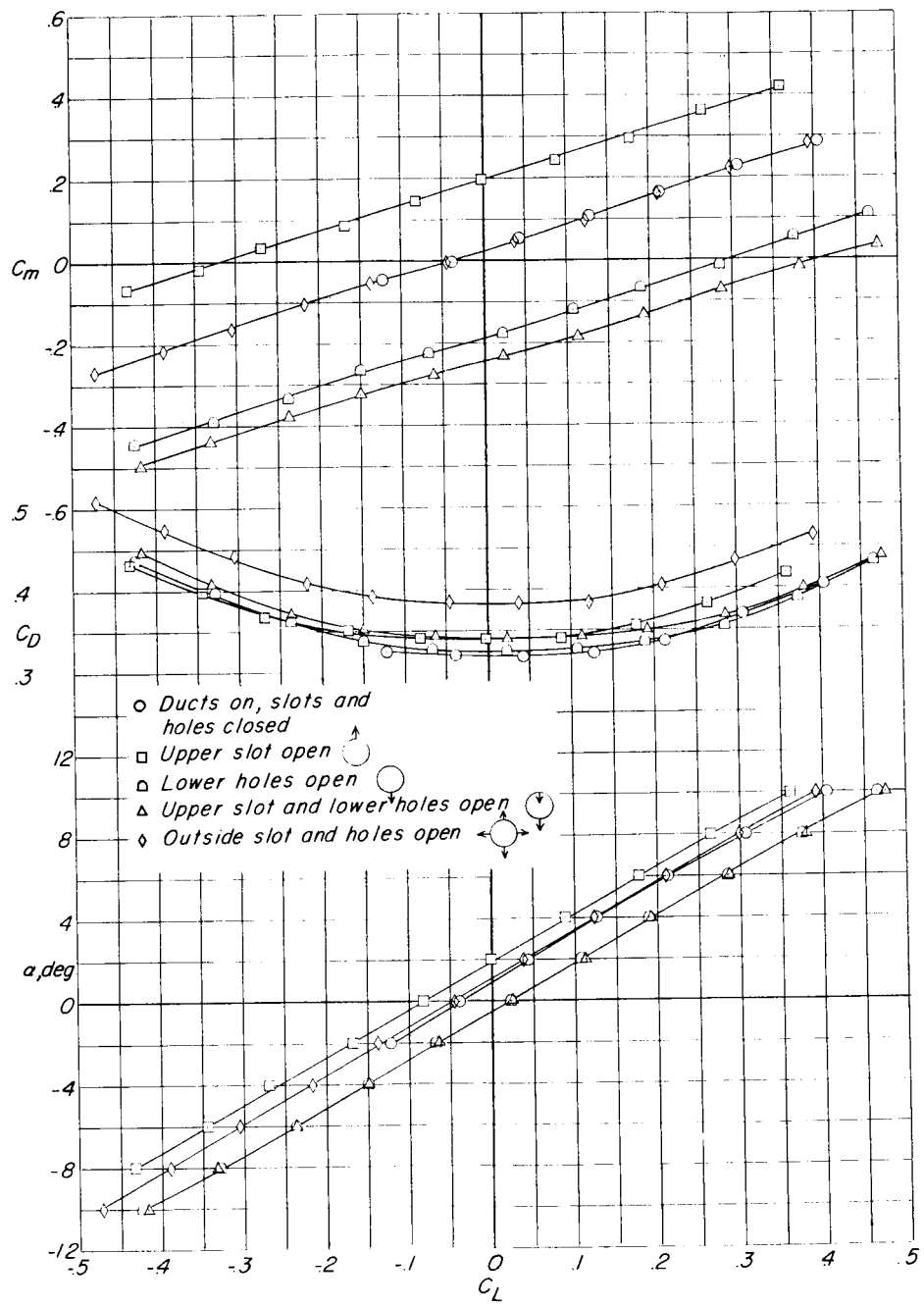

(a) M = 0.75.

Figure 5.- Effect of jet controls on aerodynamic characteristics in pitch of model 1 with 3.5-inch-wide ring tail mounted in rear position.

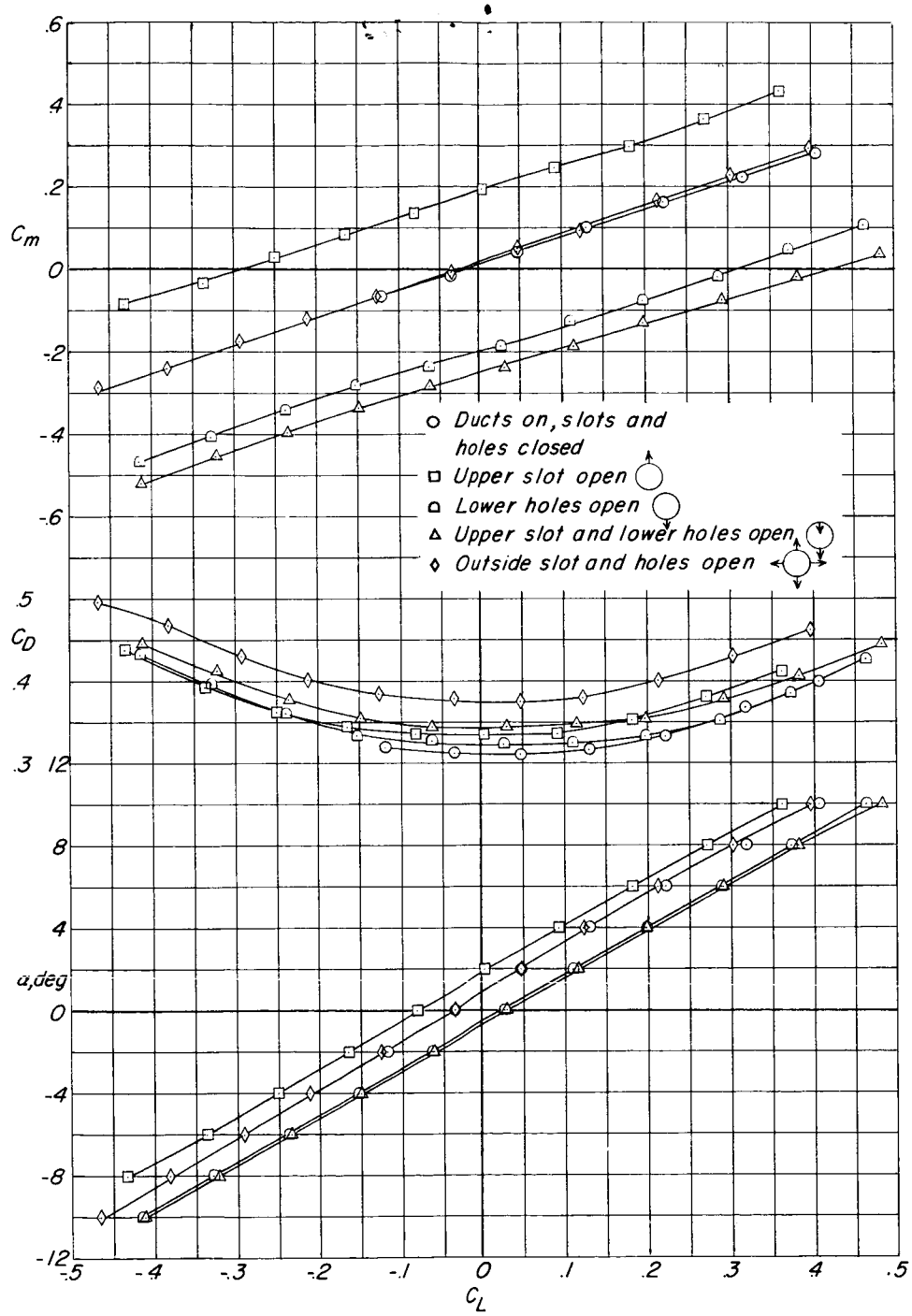

(b) M = 0.80.

Figure 5.- Continued.

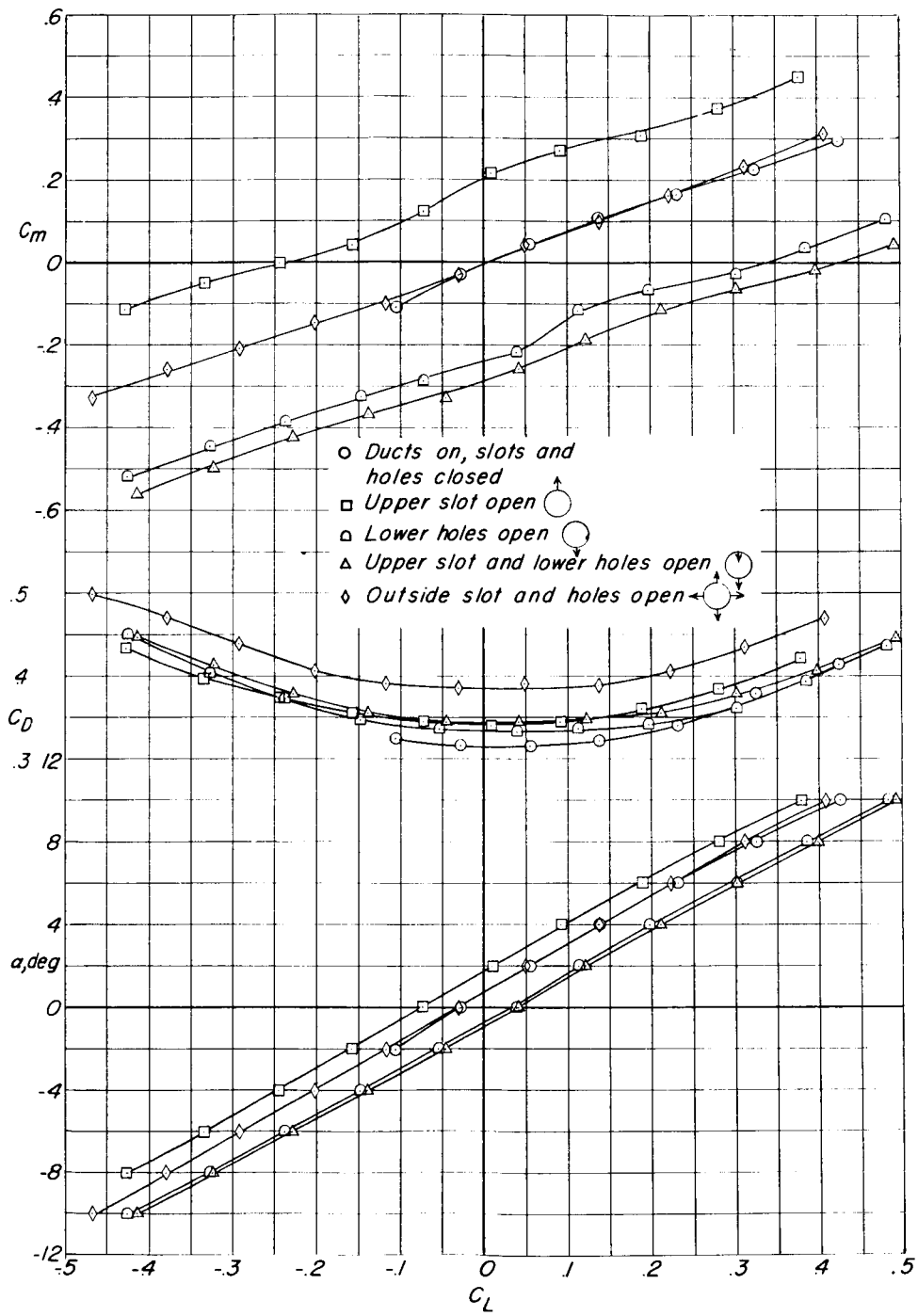

(c) M = 0.90.

Figure 5.- Concluded.

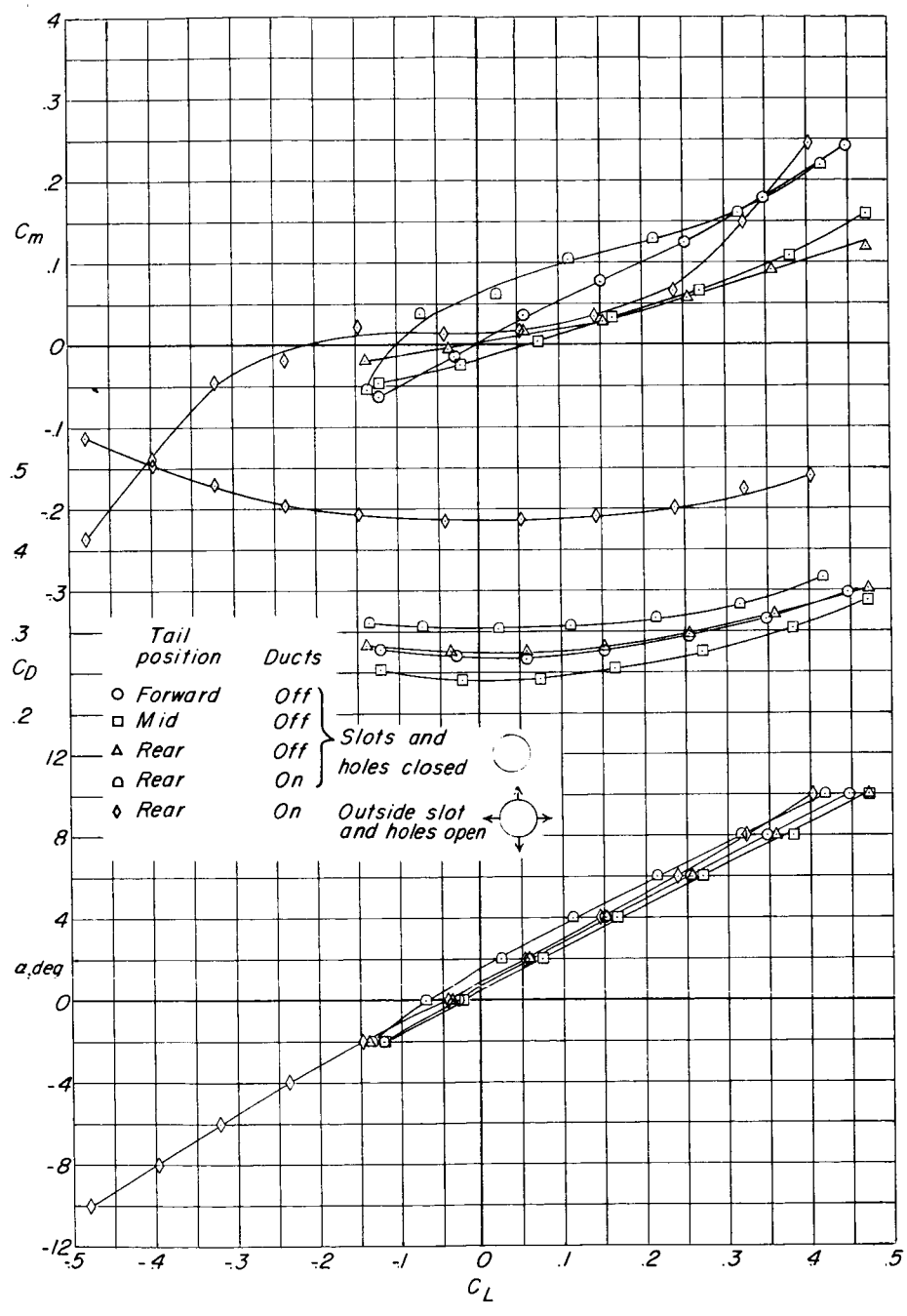

(a) M = 0.75.

Figure 6.- Effect of tail position and duct installation on aerodynamic characteristics in pitch of model 1 equipped with 2.5-inch-wide ring tail.

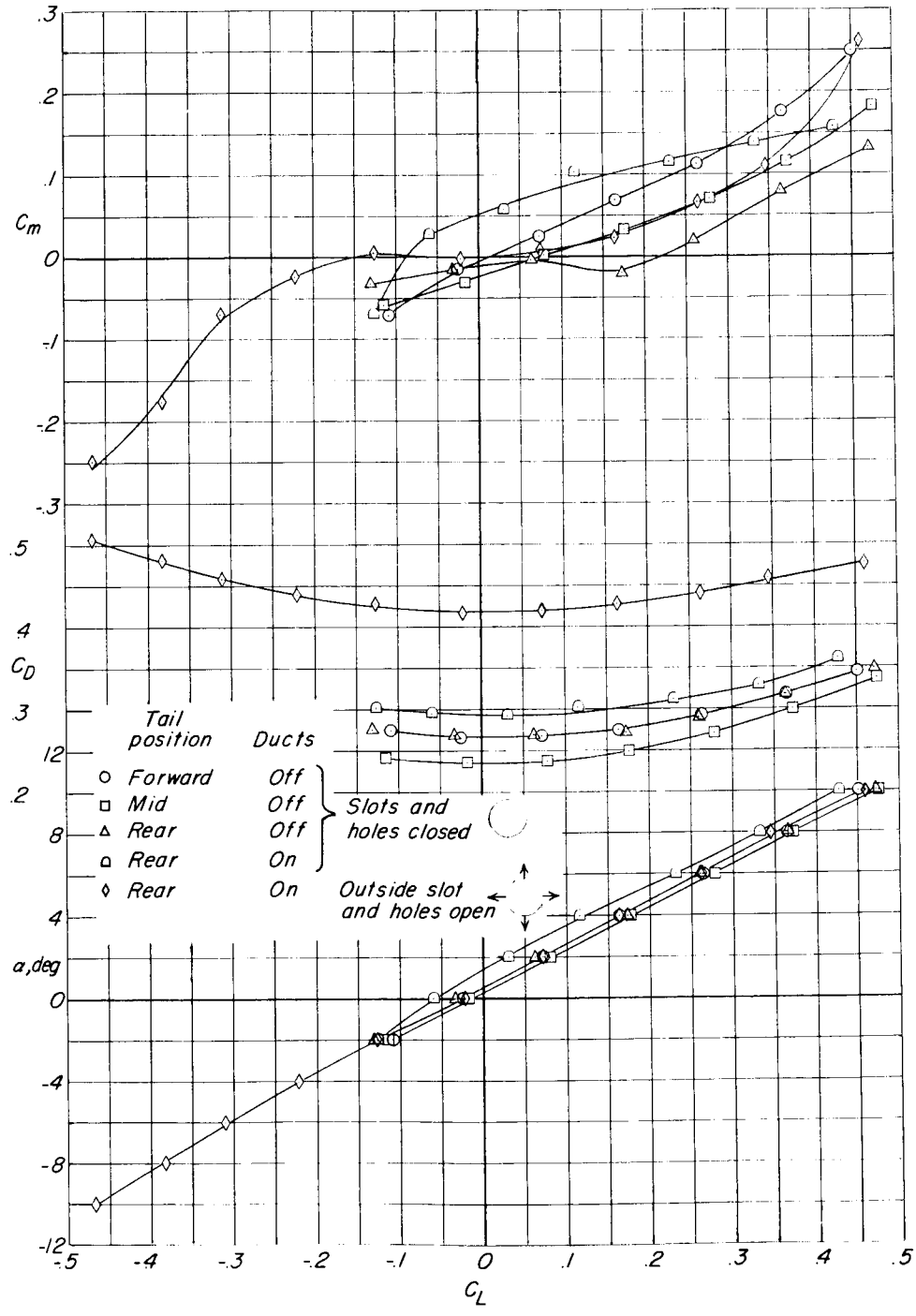

(b) M = 0.80.

Figure 6.- Continued.

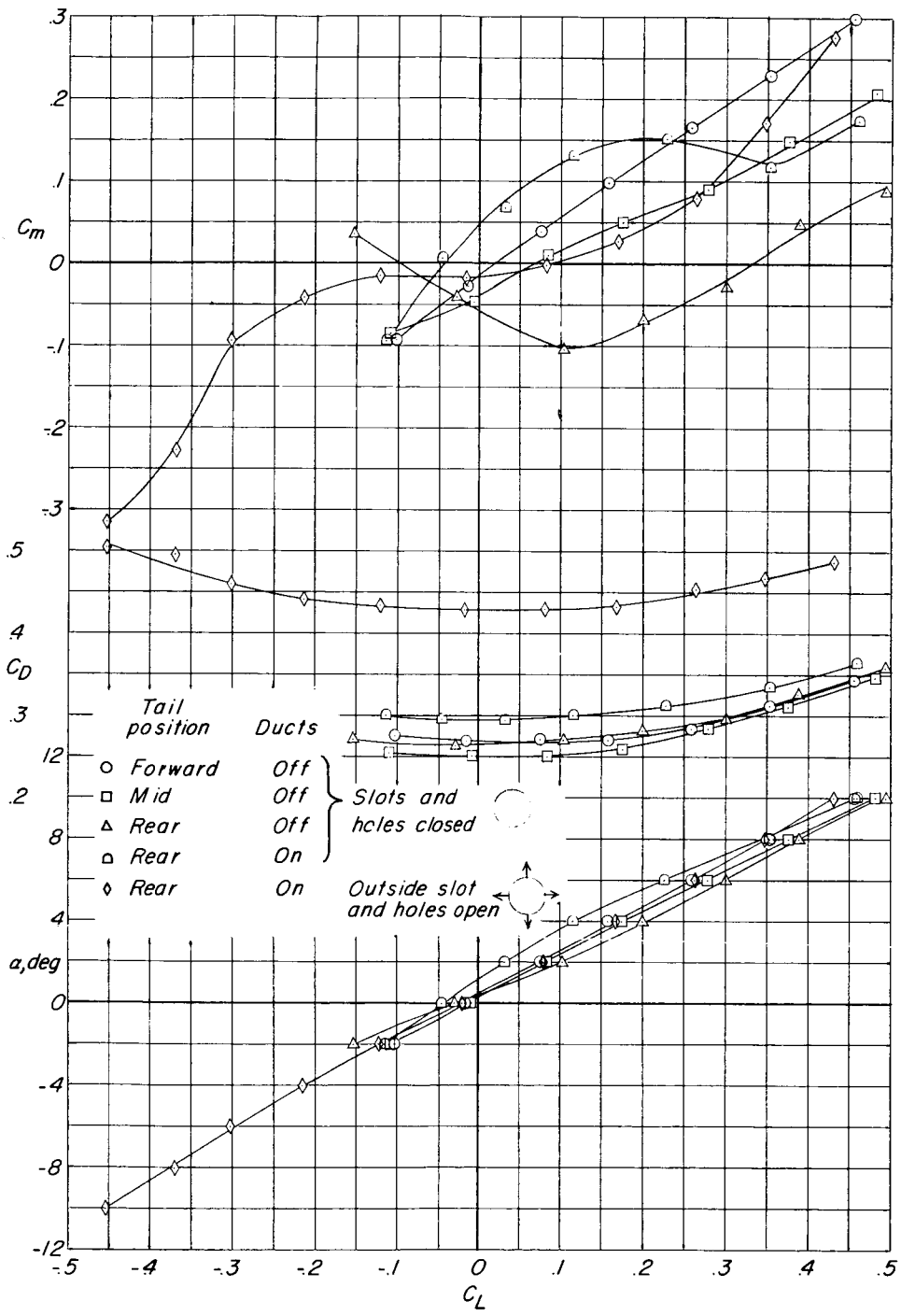

(c) M = 0.90.

Figure 6.- Concluded.

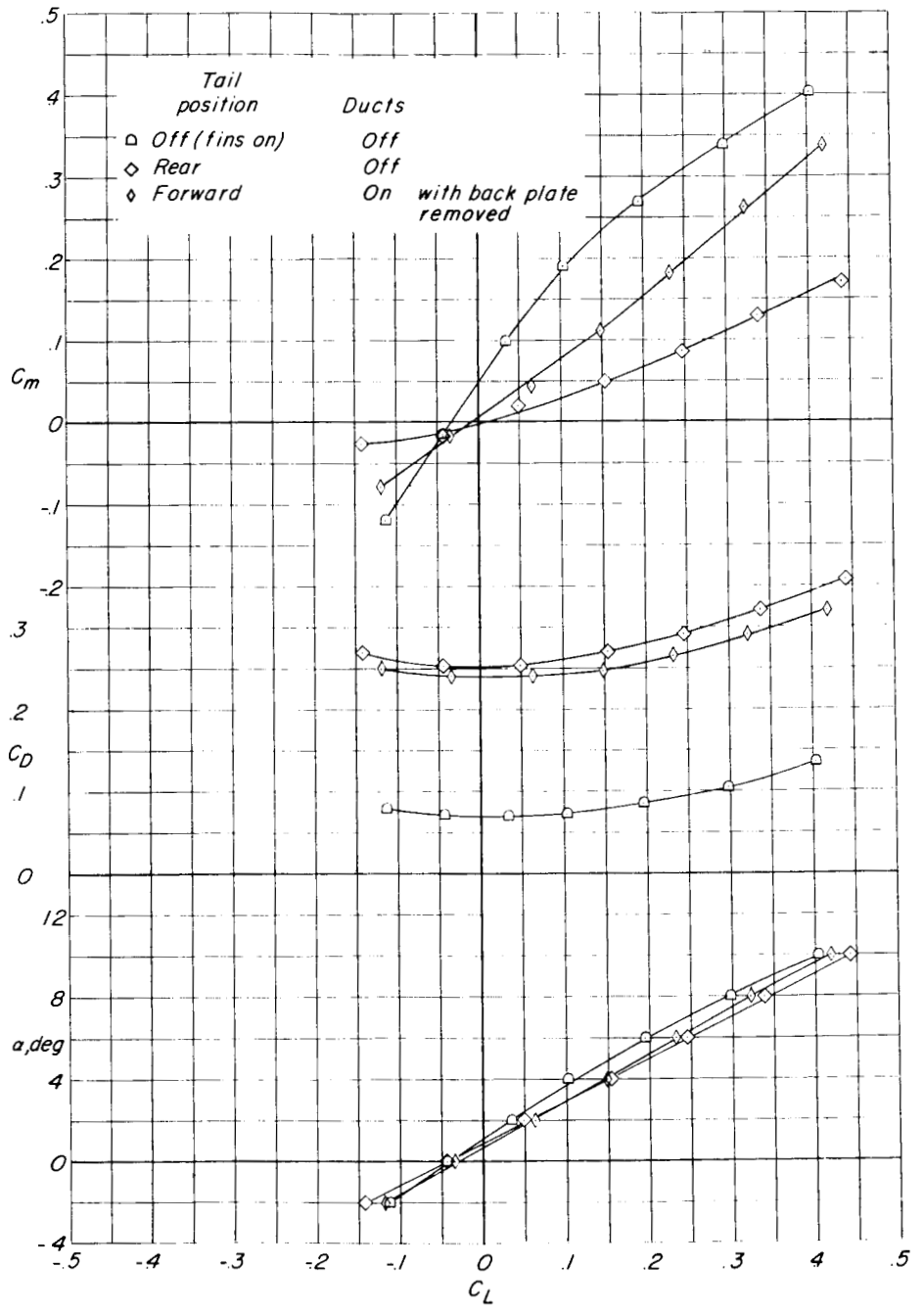

(a) M = 0.75.

Figure 7.- Aerodynamic characteristics in pitch of model 1 with ring tail off (fins on) and with 3.5-inch-wide tail on with ducts open at rear.

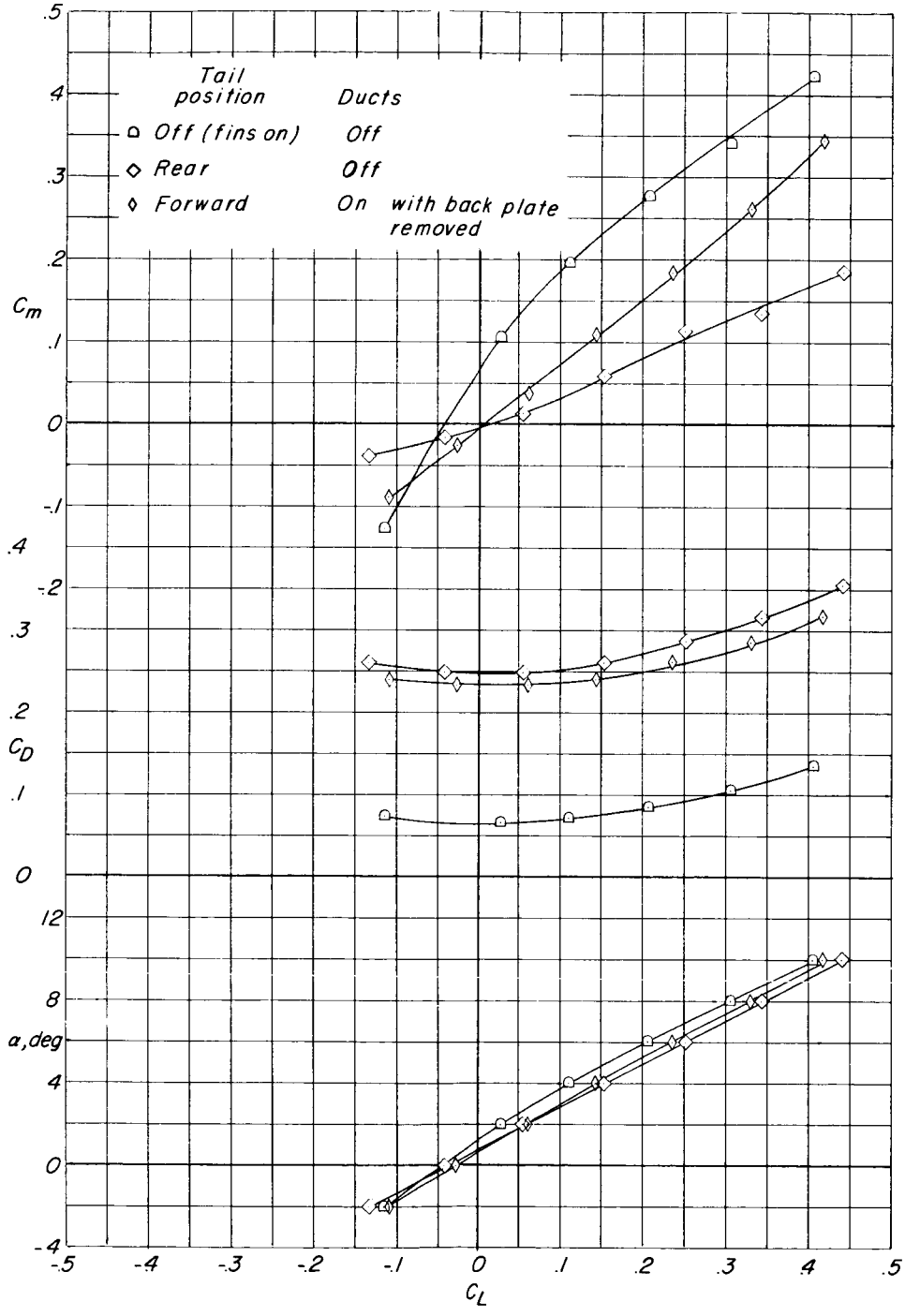

(b) M = 0.80.

Figure 7.- Continued.

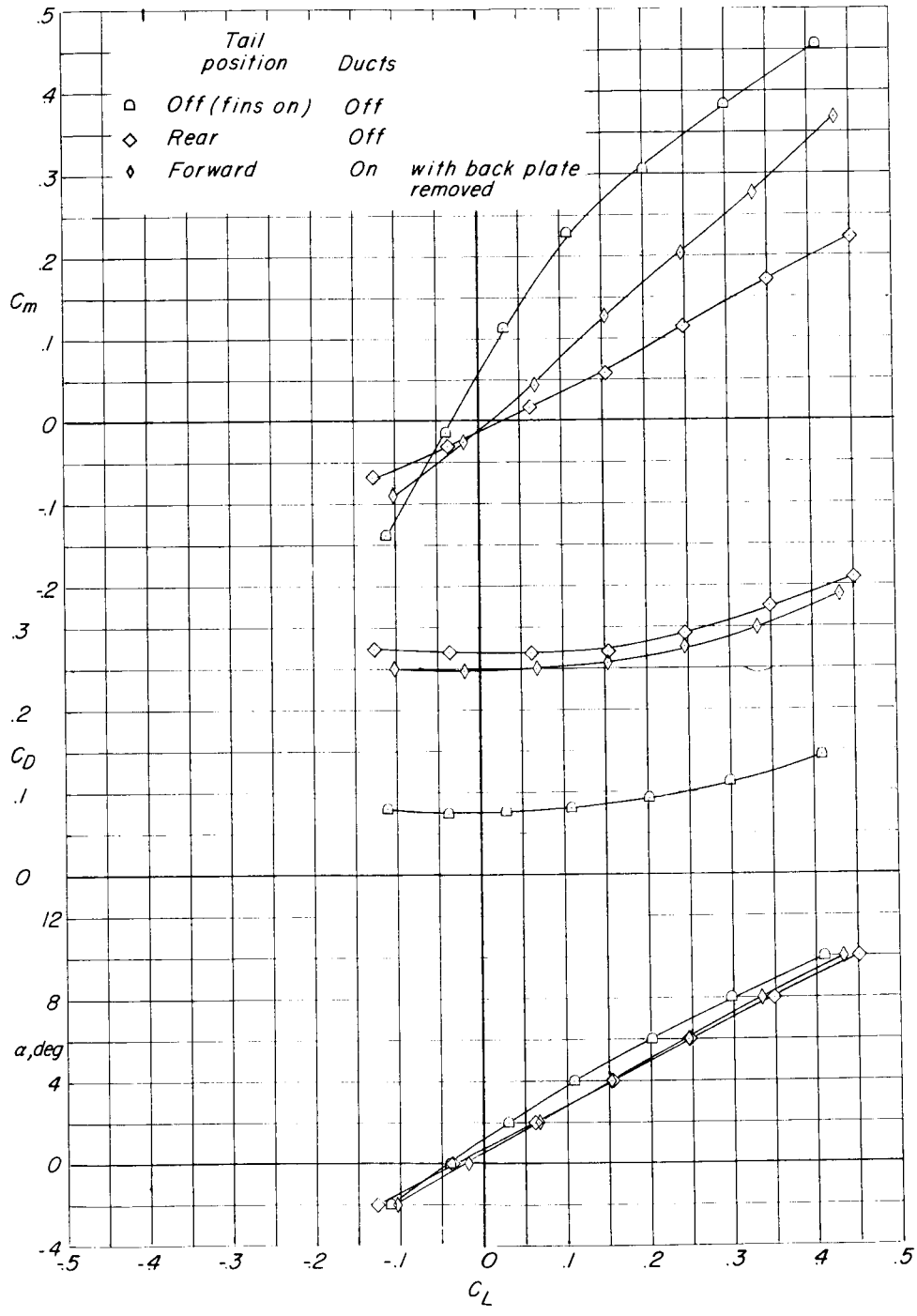

(c) M = 0.90.

Figure 7.- Concluded.

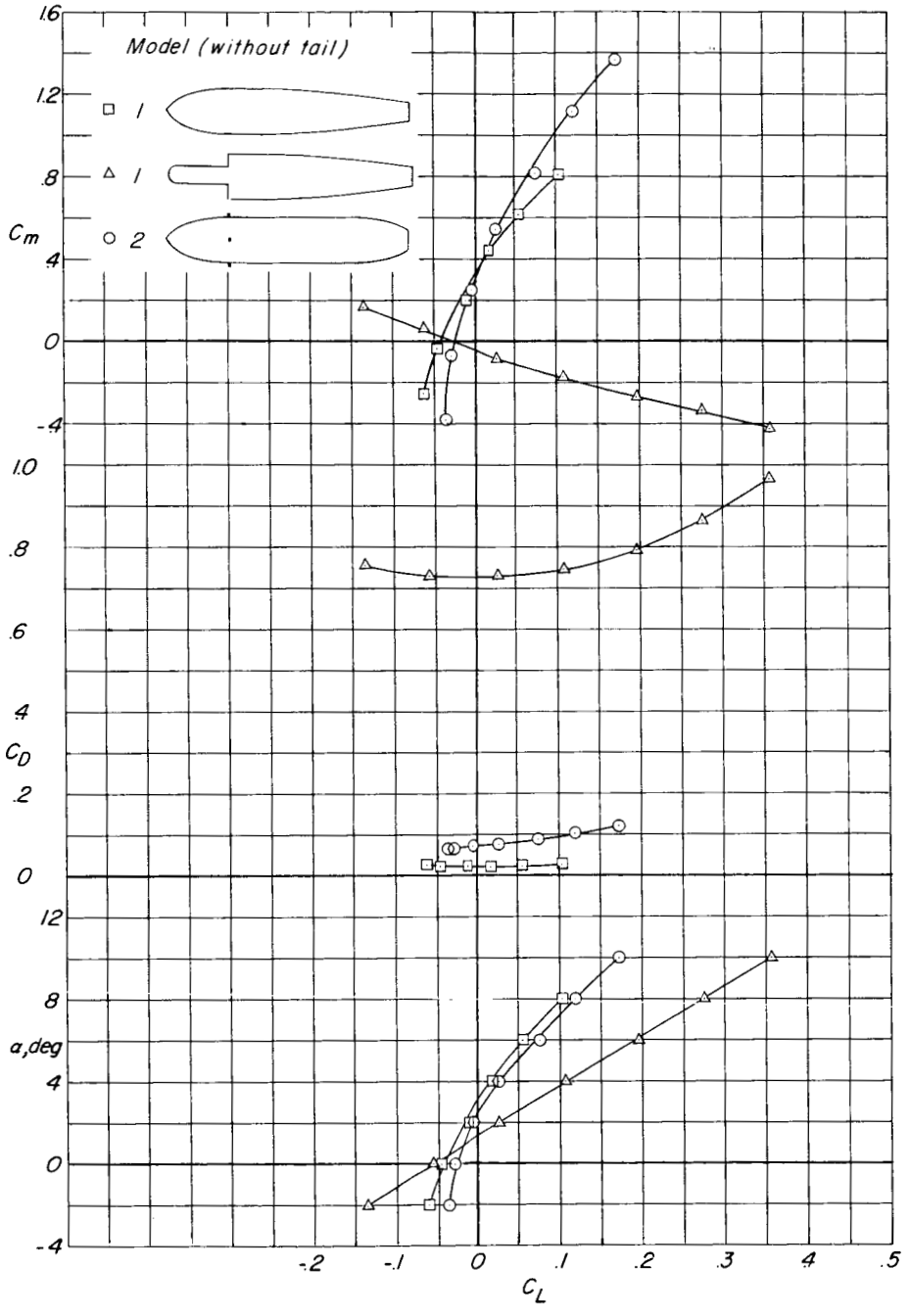

(a) M = 0.75.

Figure 8.- Body-alone aerodynamic characteristics in pitch of models 1 and 2.

[redacted]

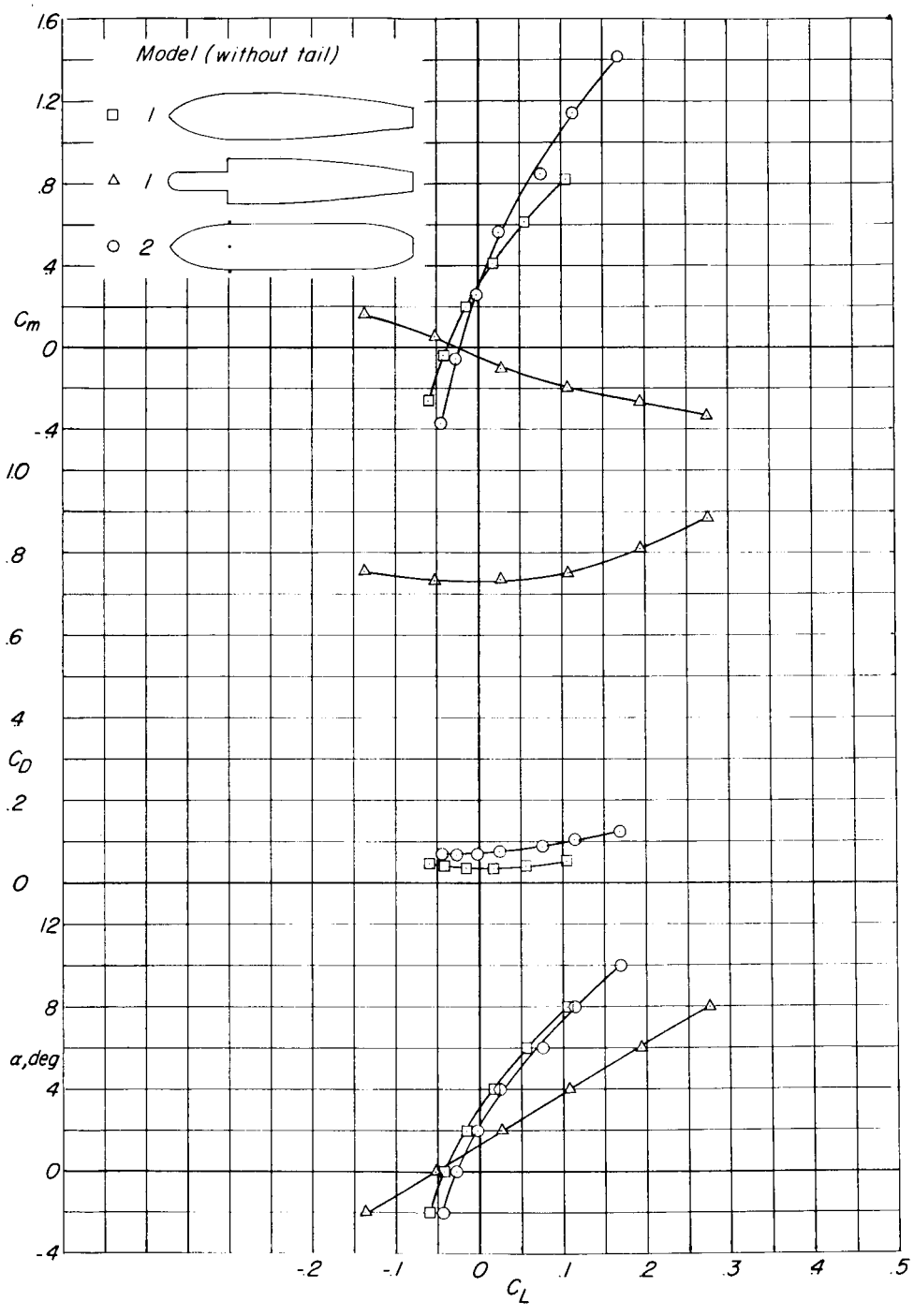

(b) M = 0.80.

Figure 8.- Continued.

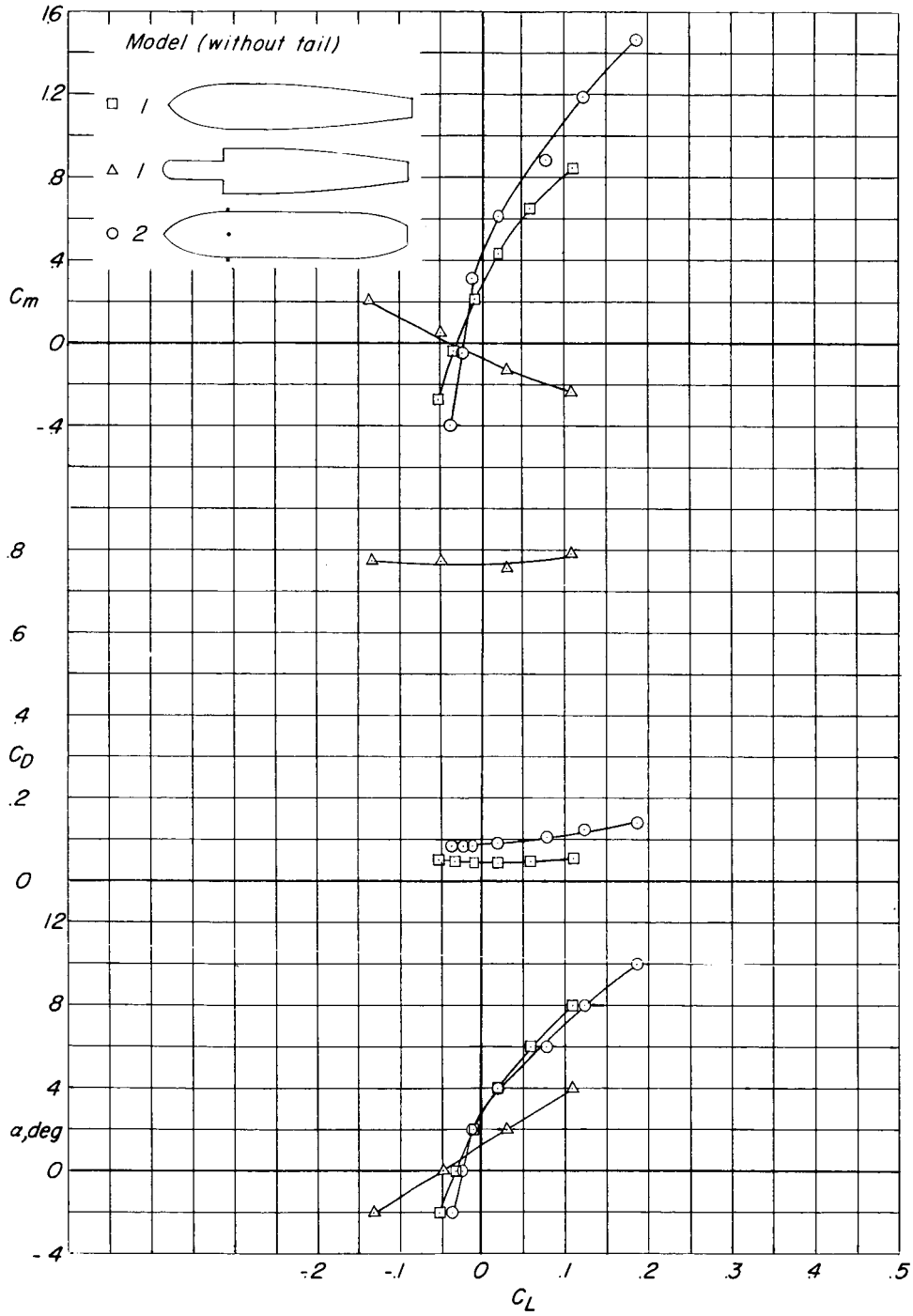

(c) M = 0.90.

Figure 8.- Concluded.

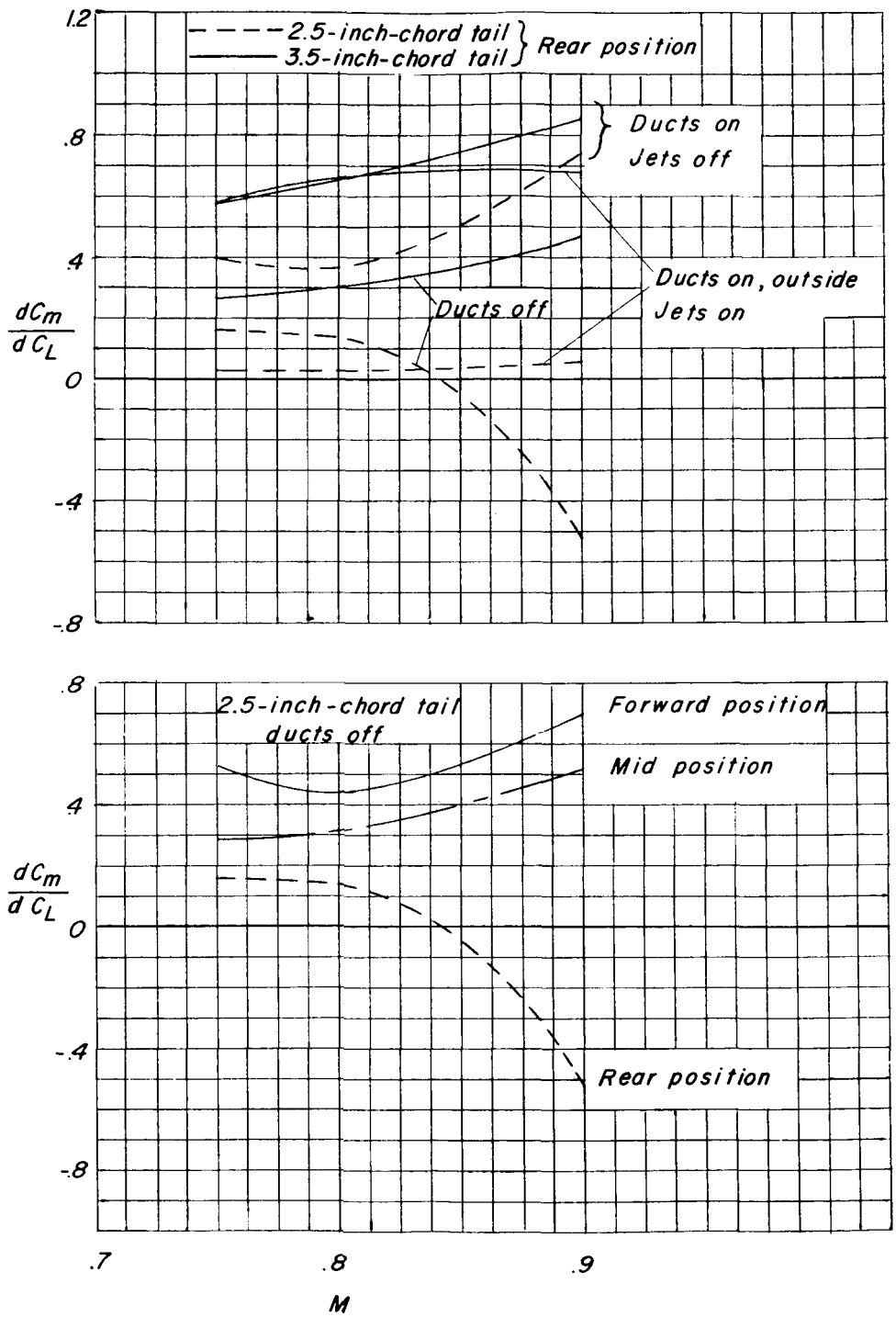

Figure 9.- Summary of effects of ducts, ring-tail width, and tail position on static stability of model 1.

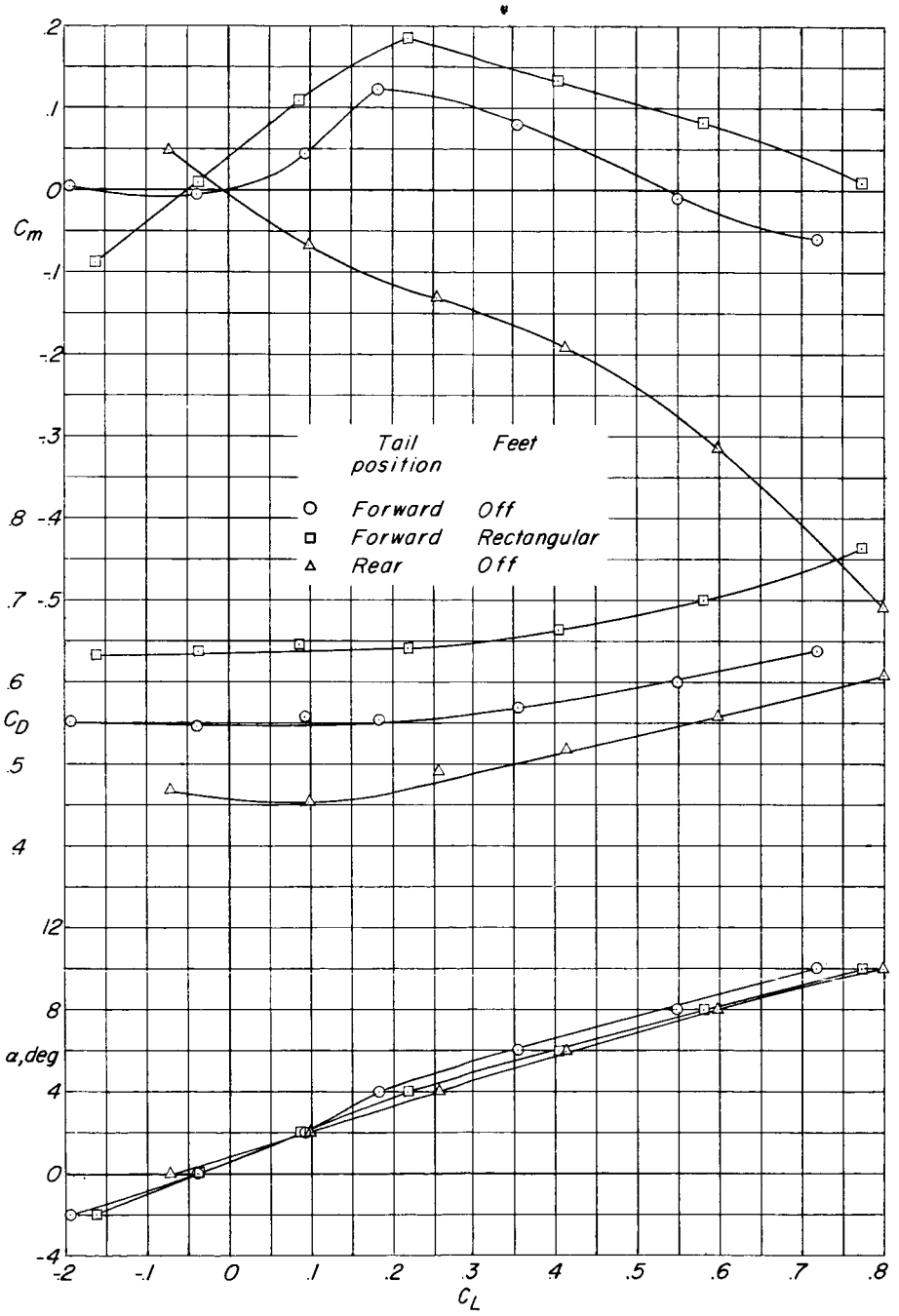

(a) M = 0.75.

Figure 10.- Effect of tail position and guide feet on aerodynamic characteristics in pitch of model 2 with 7-inch-diameter ring tail.

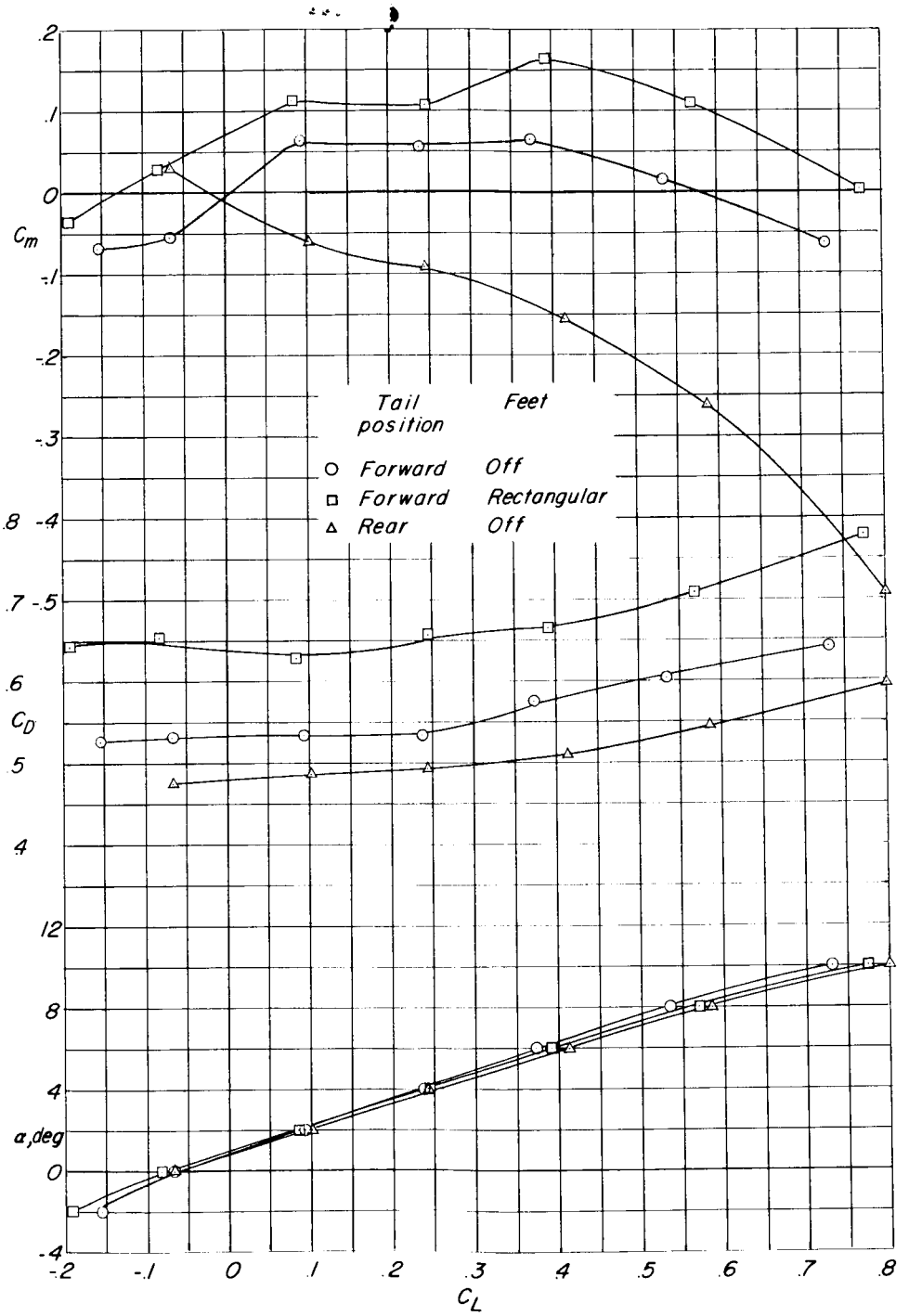

(b) M = 0.80.

Figure 10.- Continued.

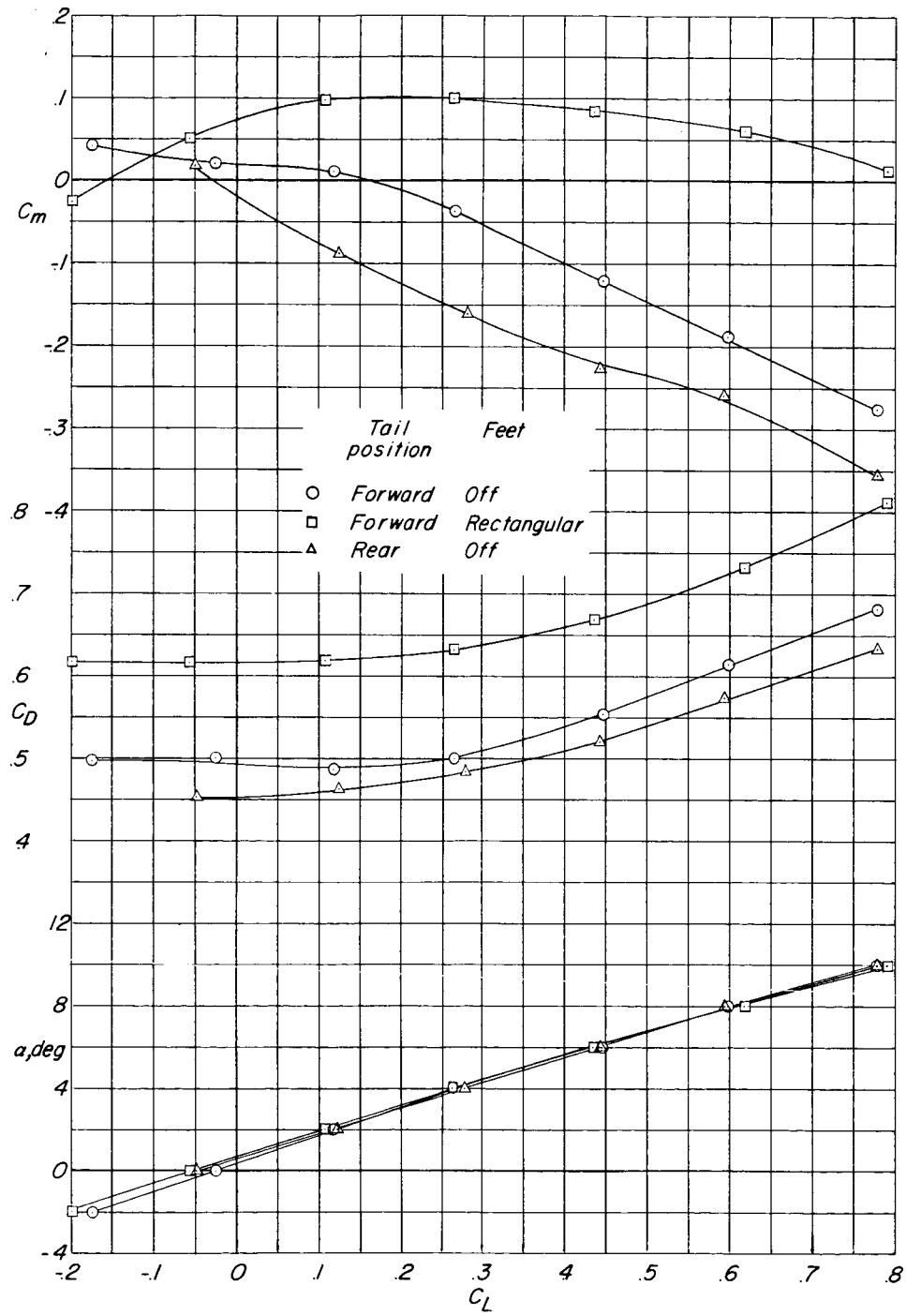

(c) M = 0.90.

Figure 10.- Concluded.

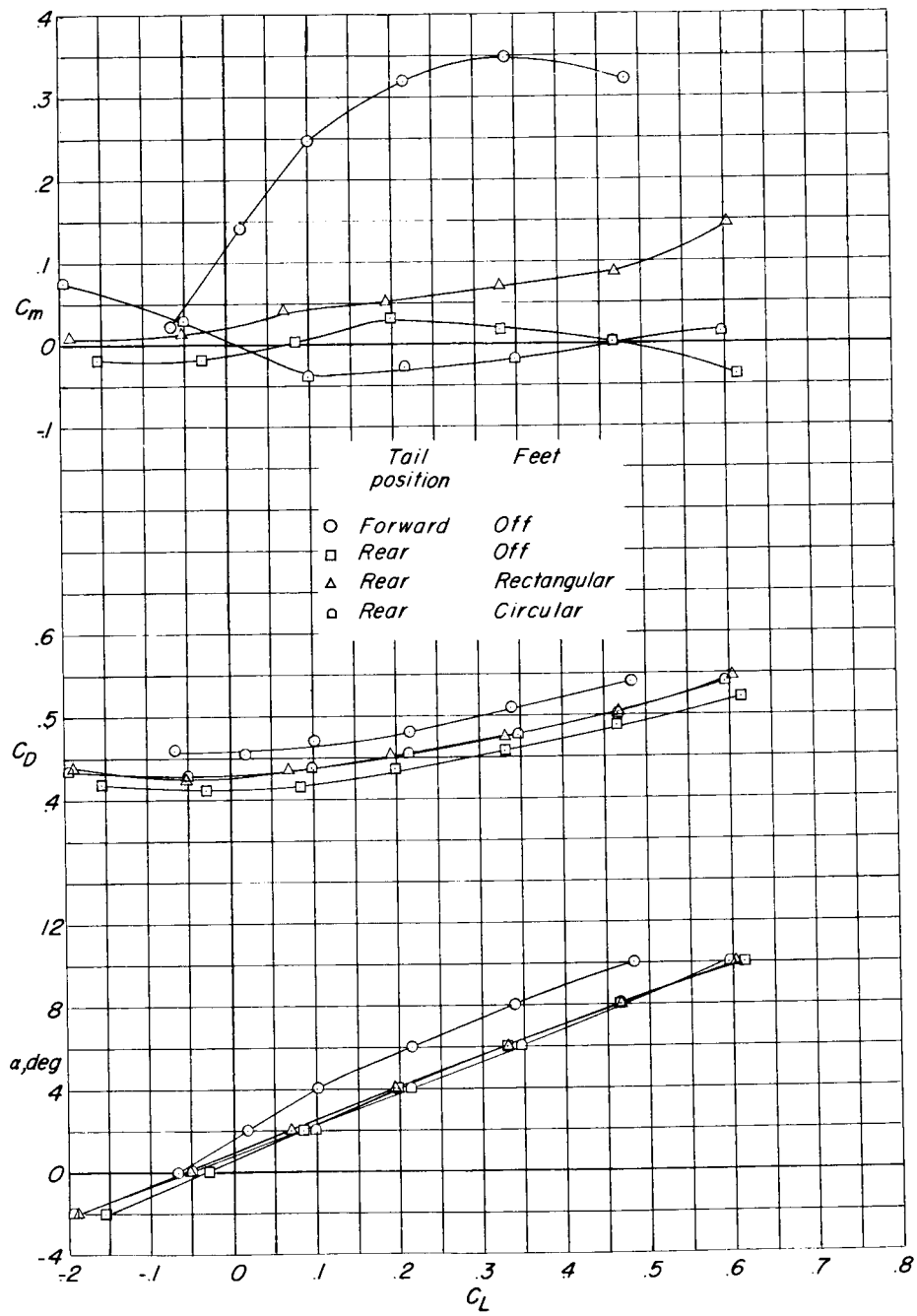

(a) M = 0.75.

Figure 11.- Effect of tail position and guide feet on aerodynamic characteristics in pitch of model 2 with 6-inch-diameter ring tail.

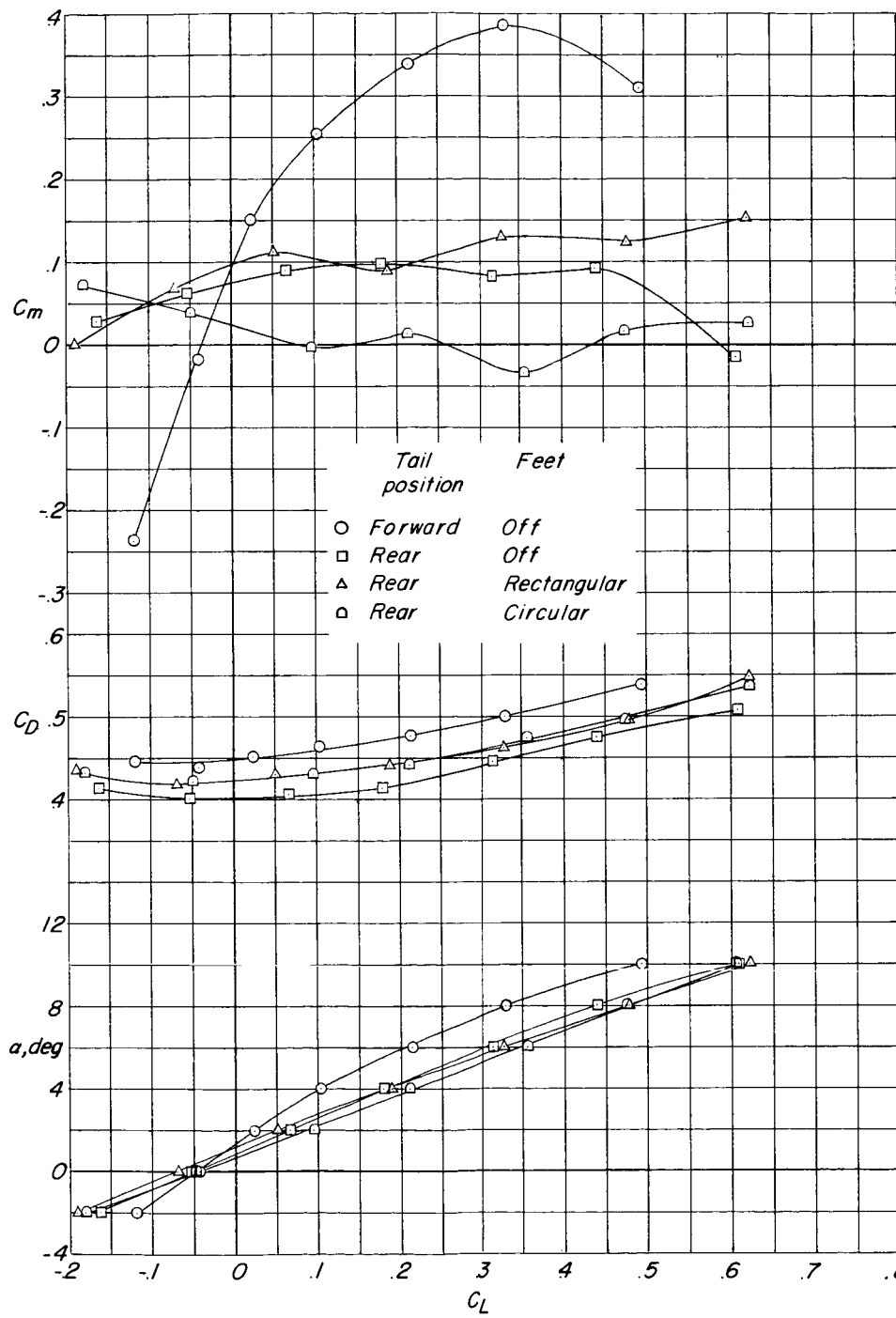

(b) M = 0.80.

Figure 11.- Continued.

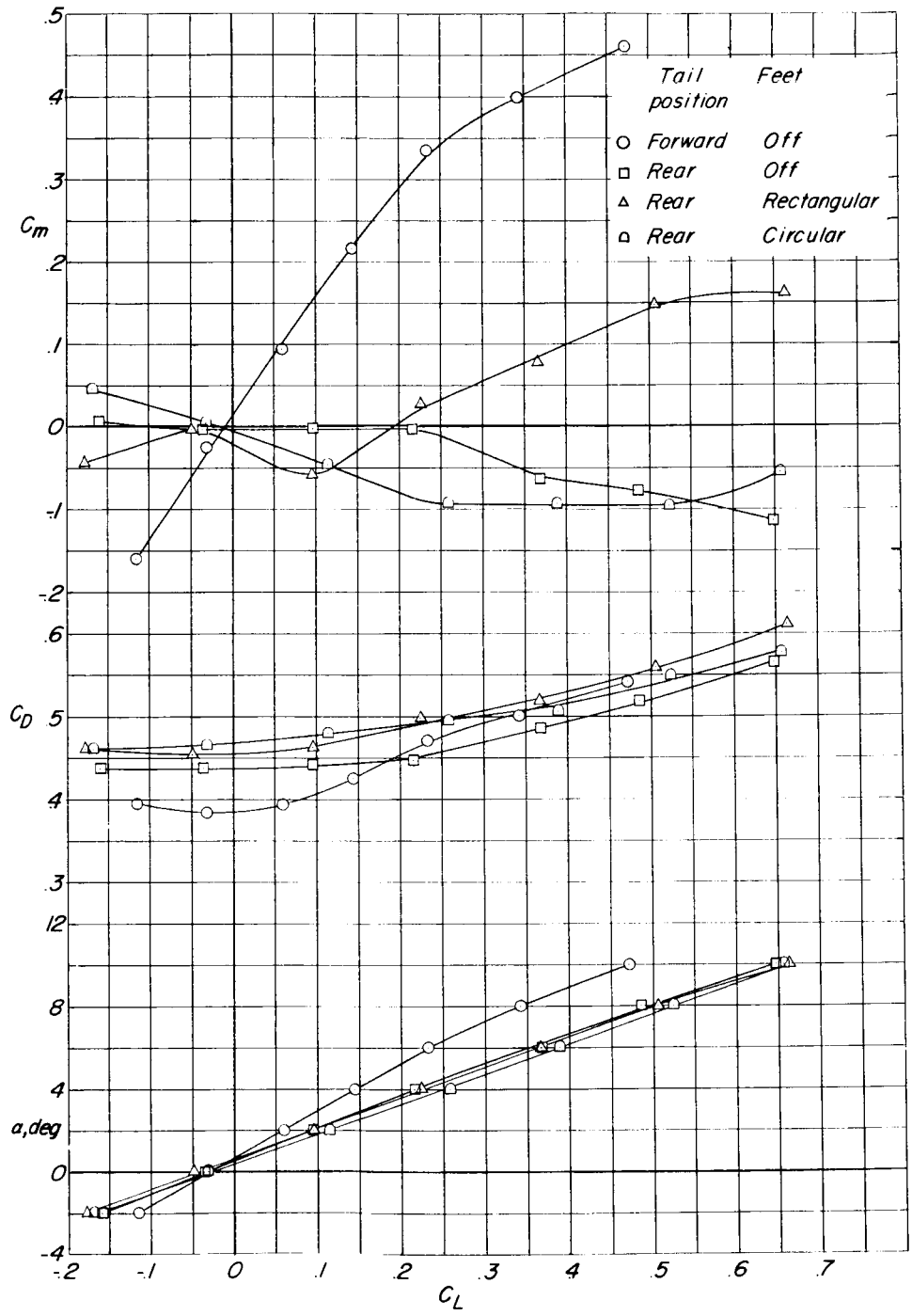

(c) M = 0.90.

Figure 11.- Concluded.

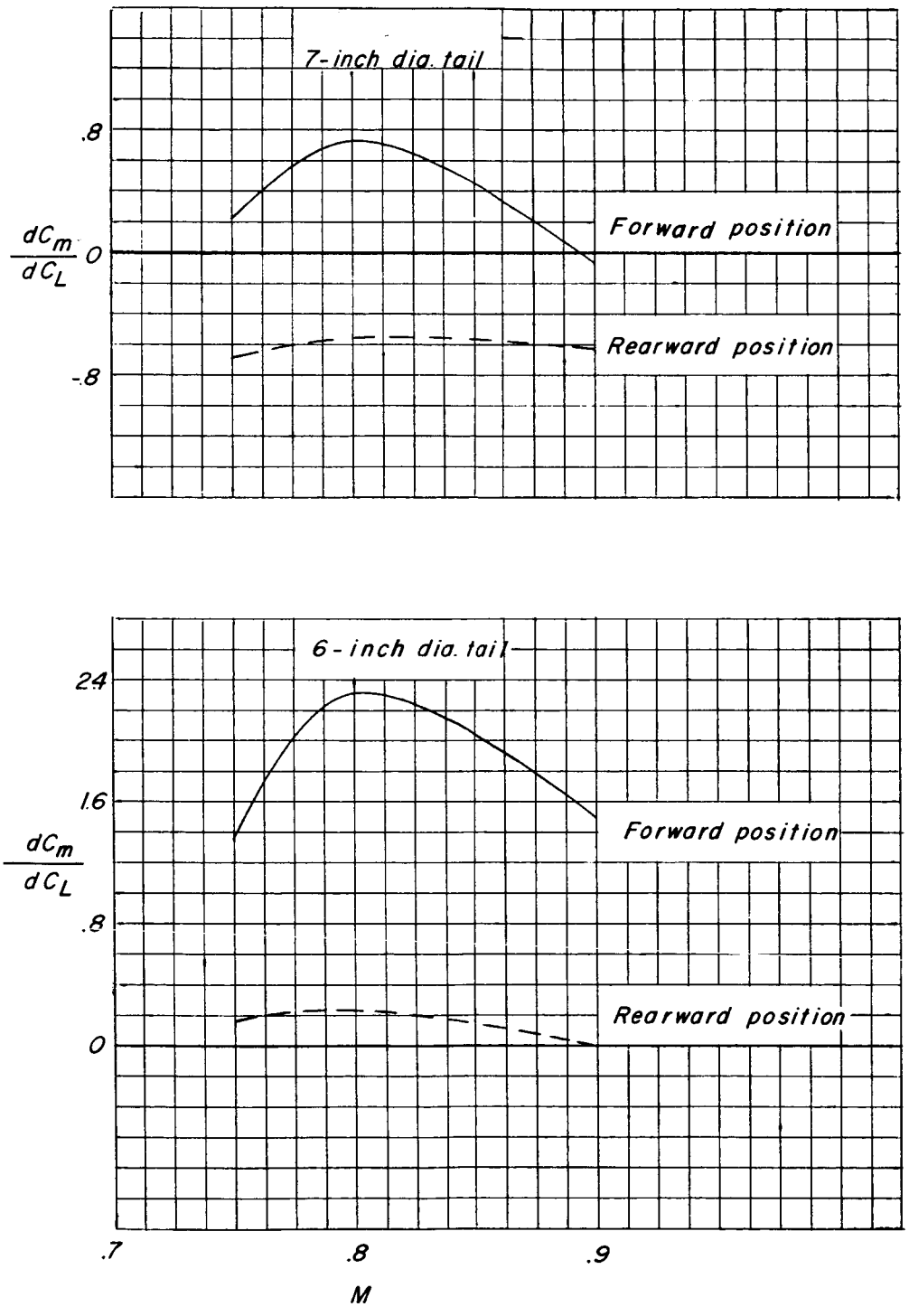

Figure 12.- Summary of effects of tail position and ring-tail diameter on the static stability of model 2. Guide feet off.

L-622

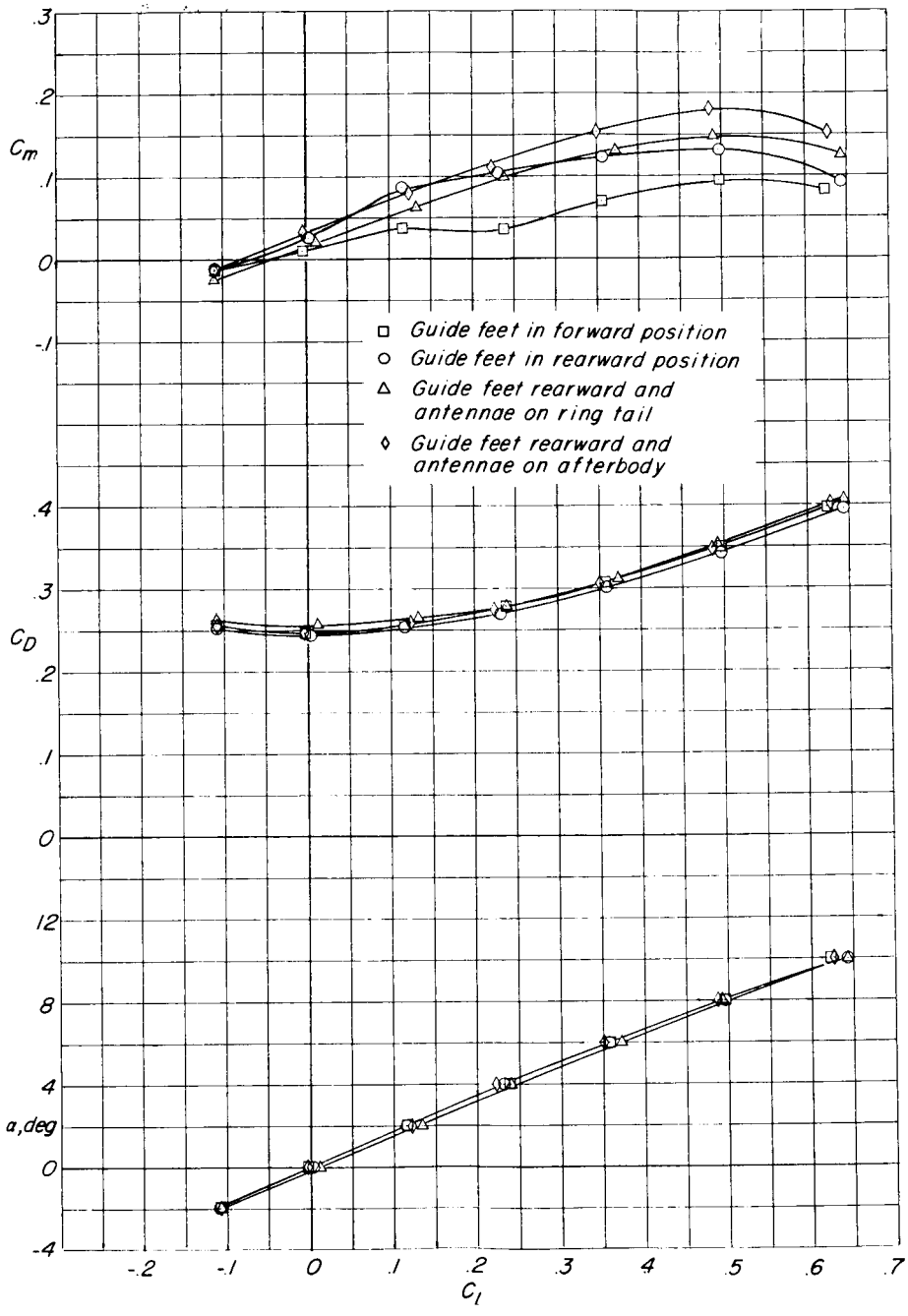

(a) M = 0.75.

Figure 13.- Effect of guide feet and antenna positions on aerodynamic characteristics in pitch of model 3 with ducts off.

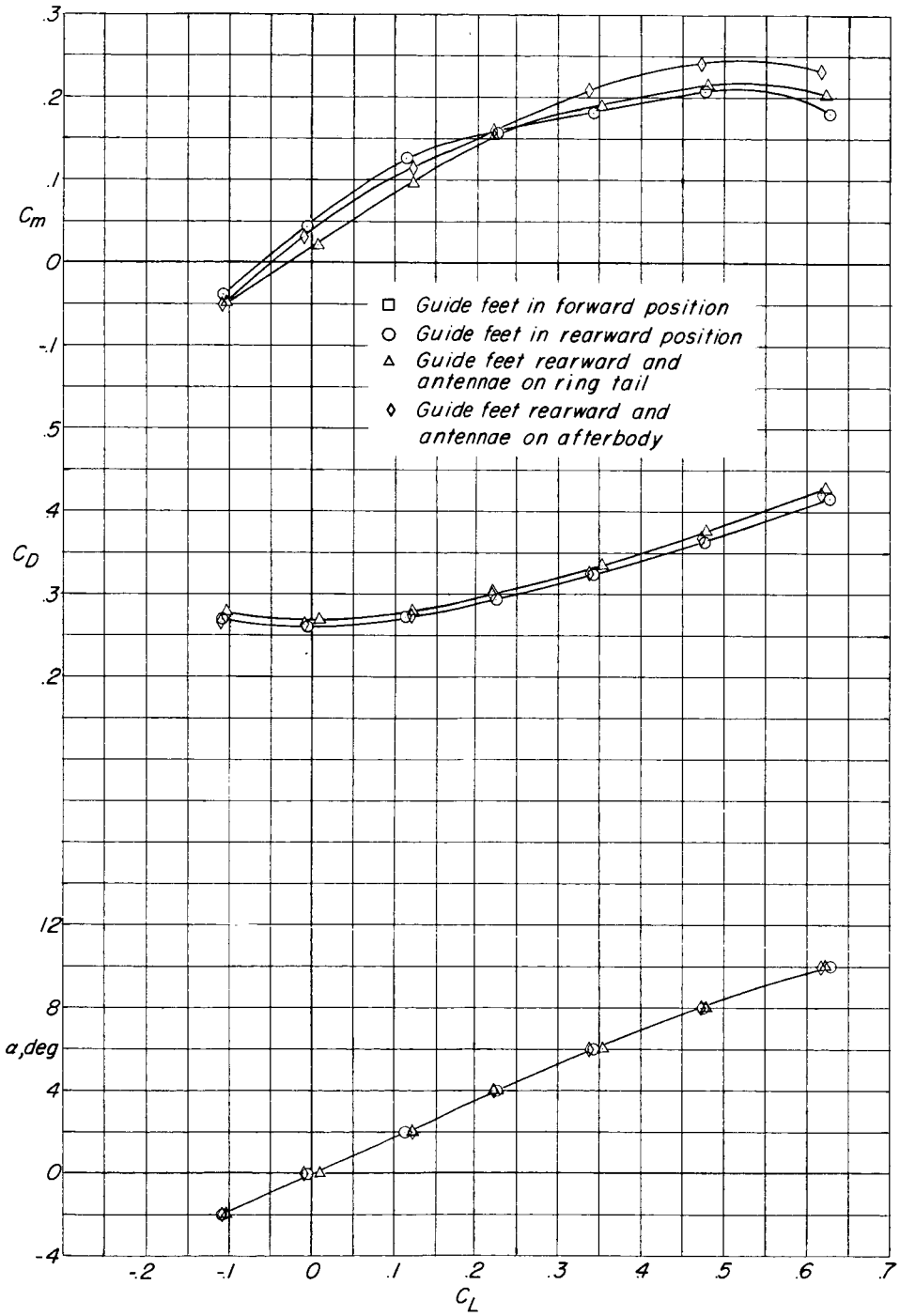

(b) M = 0.85.

Figure 13.- Continued.

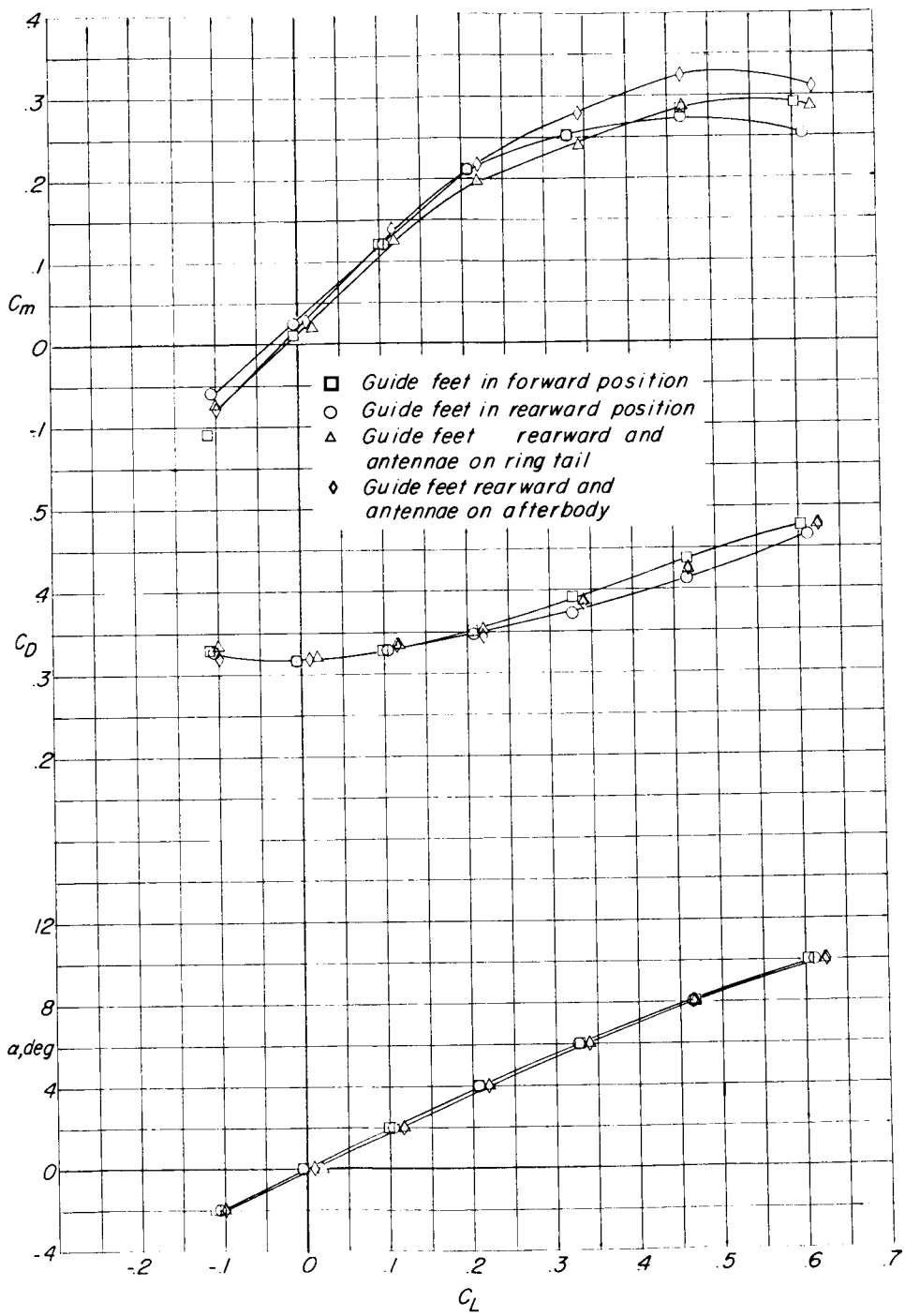

(c) M = 0.90.

Figure 13.- Concluded.

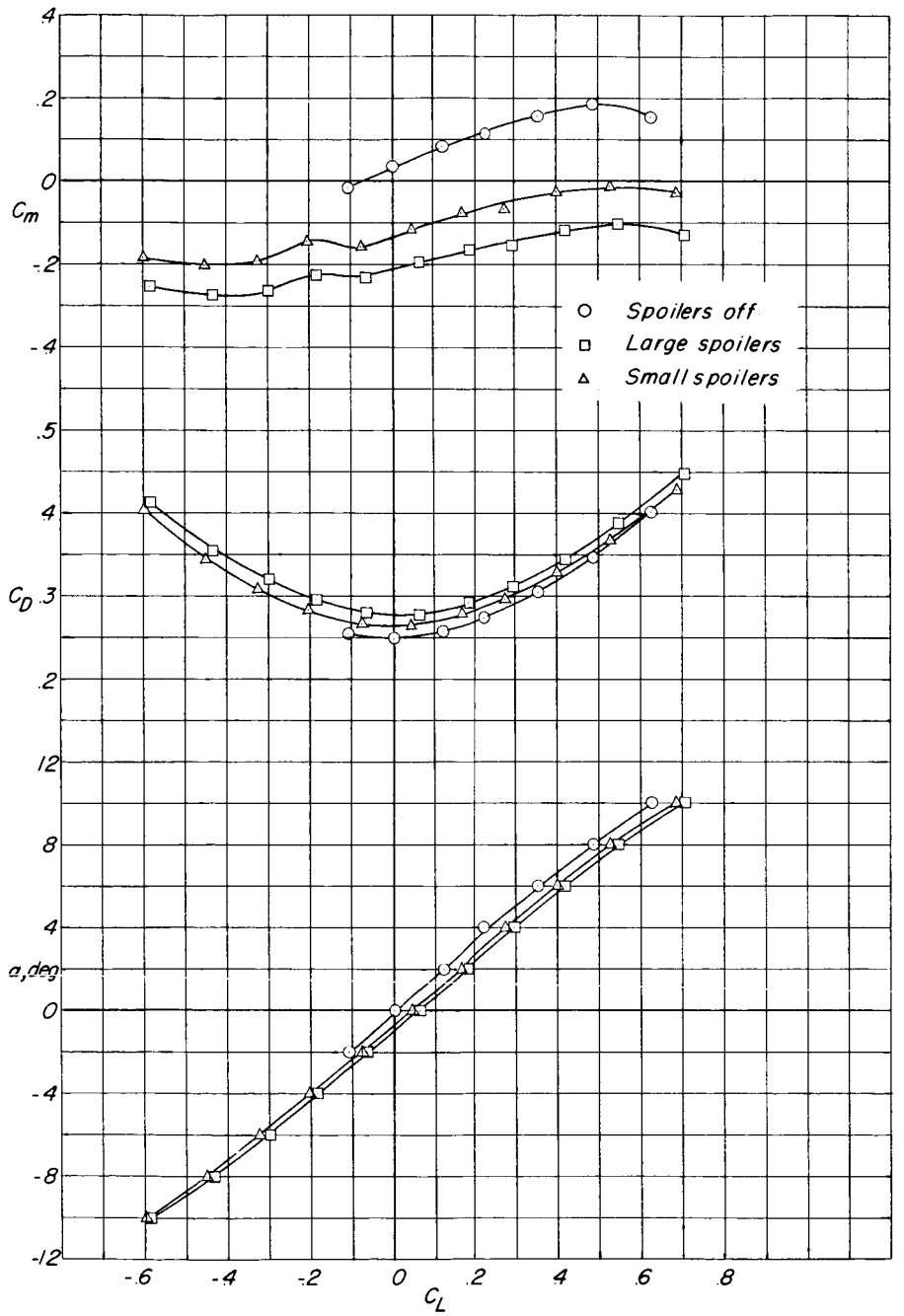

(a) M = 0.75.

Figure 14.- Effect of spoilers on the aerodynamic characteristics of model 3 with ducts off. Guide feet rearward and antennas to rear of afterbody.

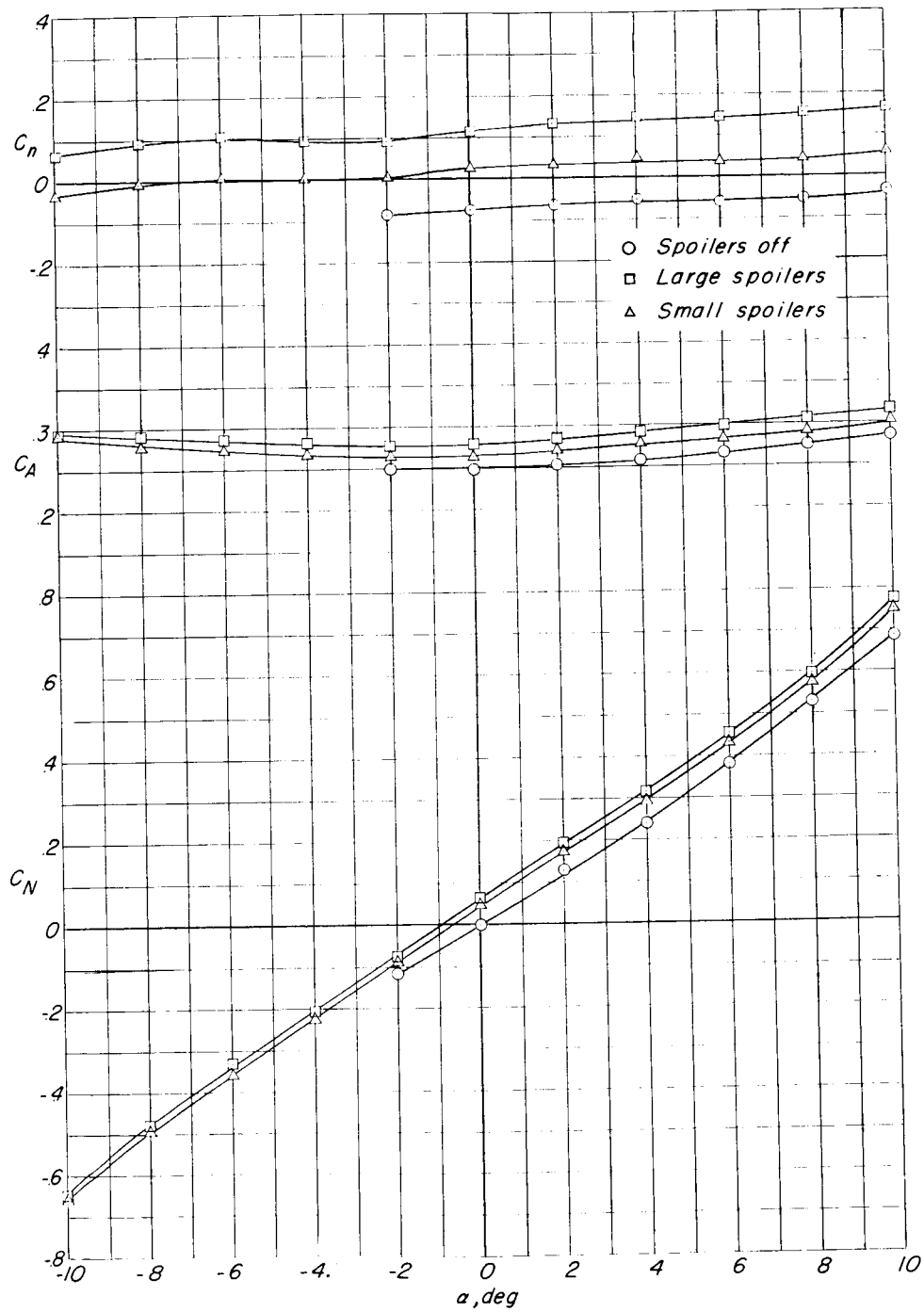

(a) M = 0.75. Concluded.

Figure 14.- Continued.

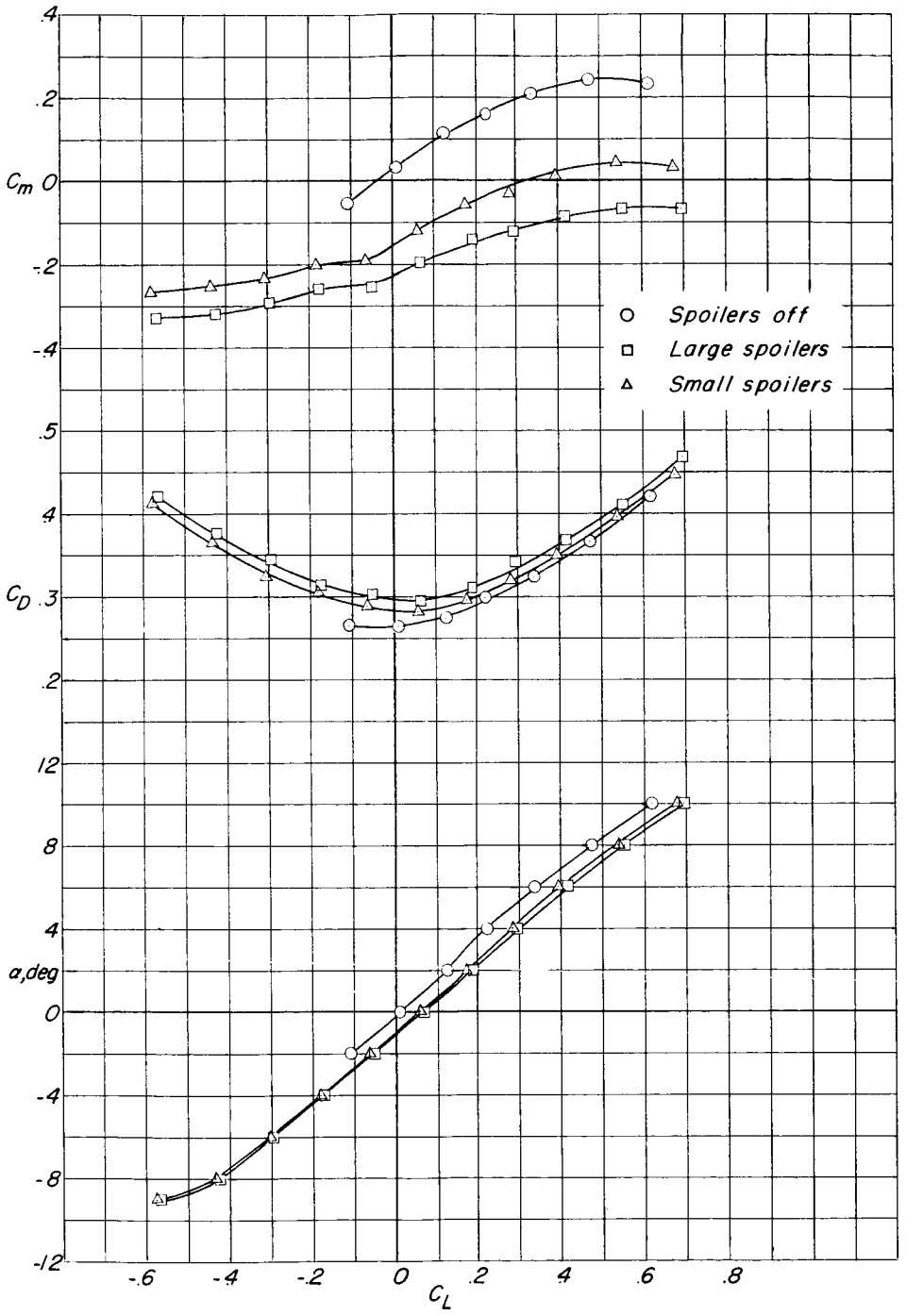

(b) M = 0.85.

Figure 14.- Continued.

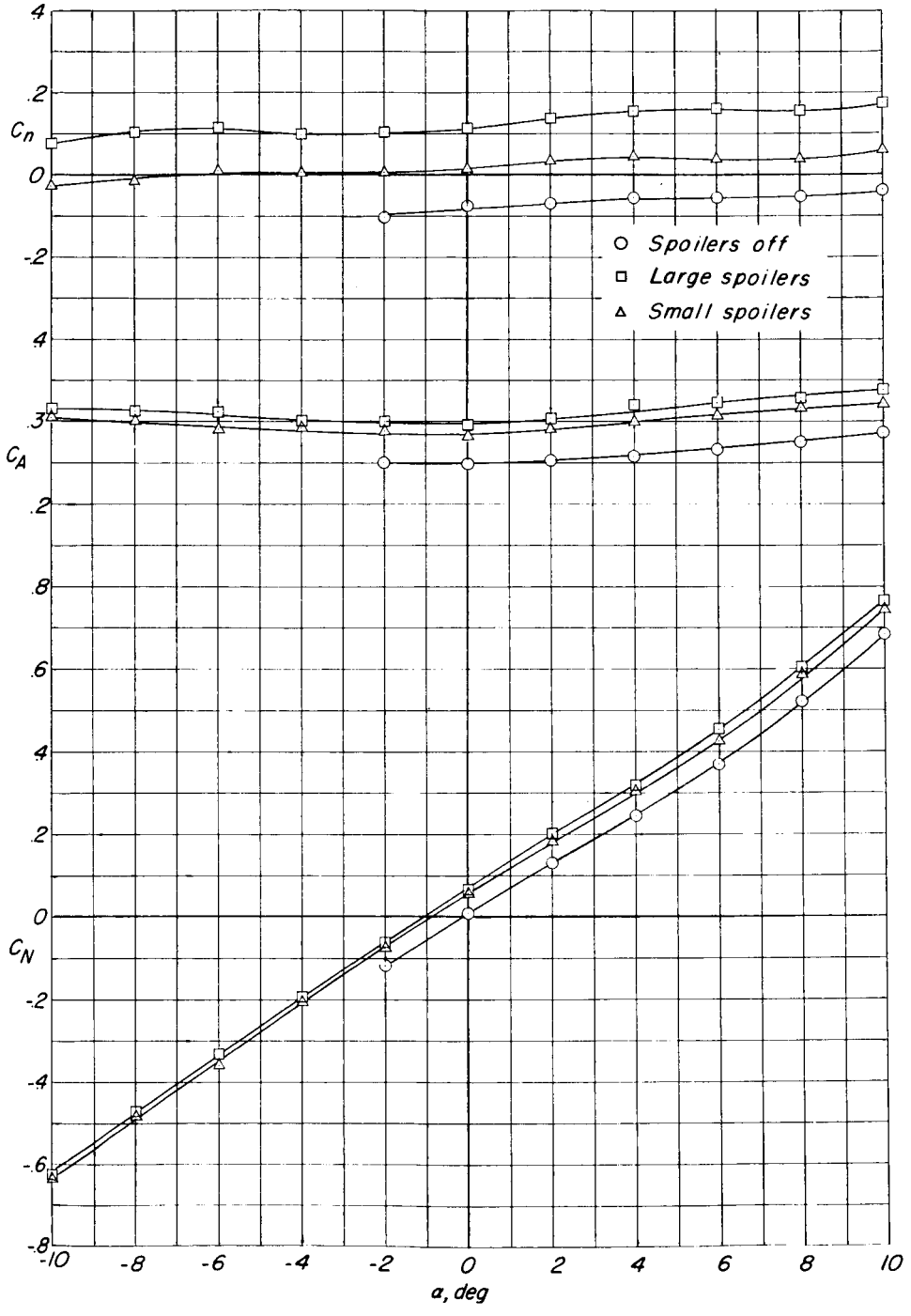

(b) M = 0.85. Concluded.

Figure 14.- Continued.

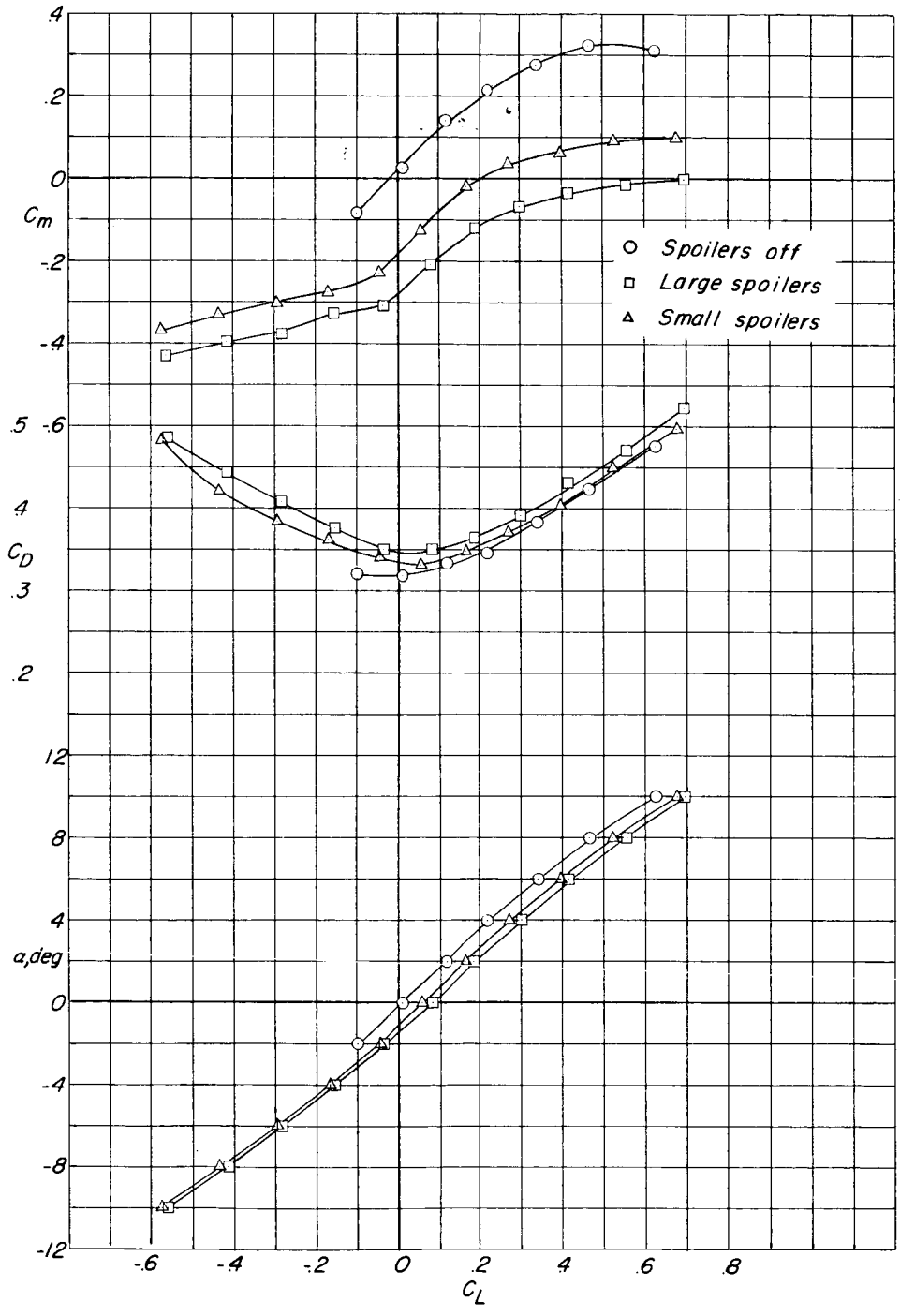

(c) M = 0.90.

Figure 14.- Continued.

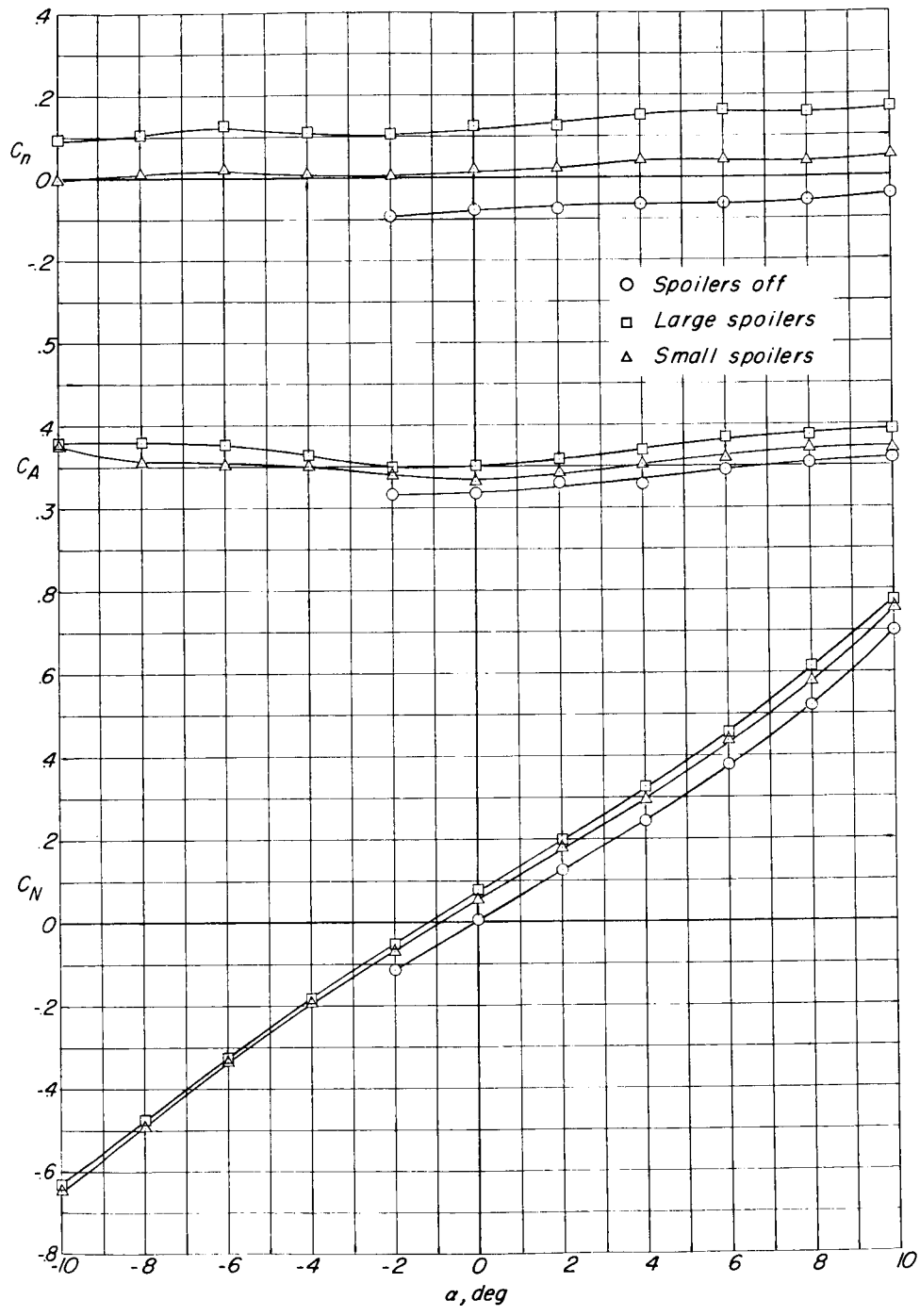

(c) M = 0.90. Concluded.

Figure 14.- Concluded.

L-622

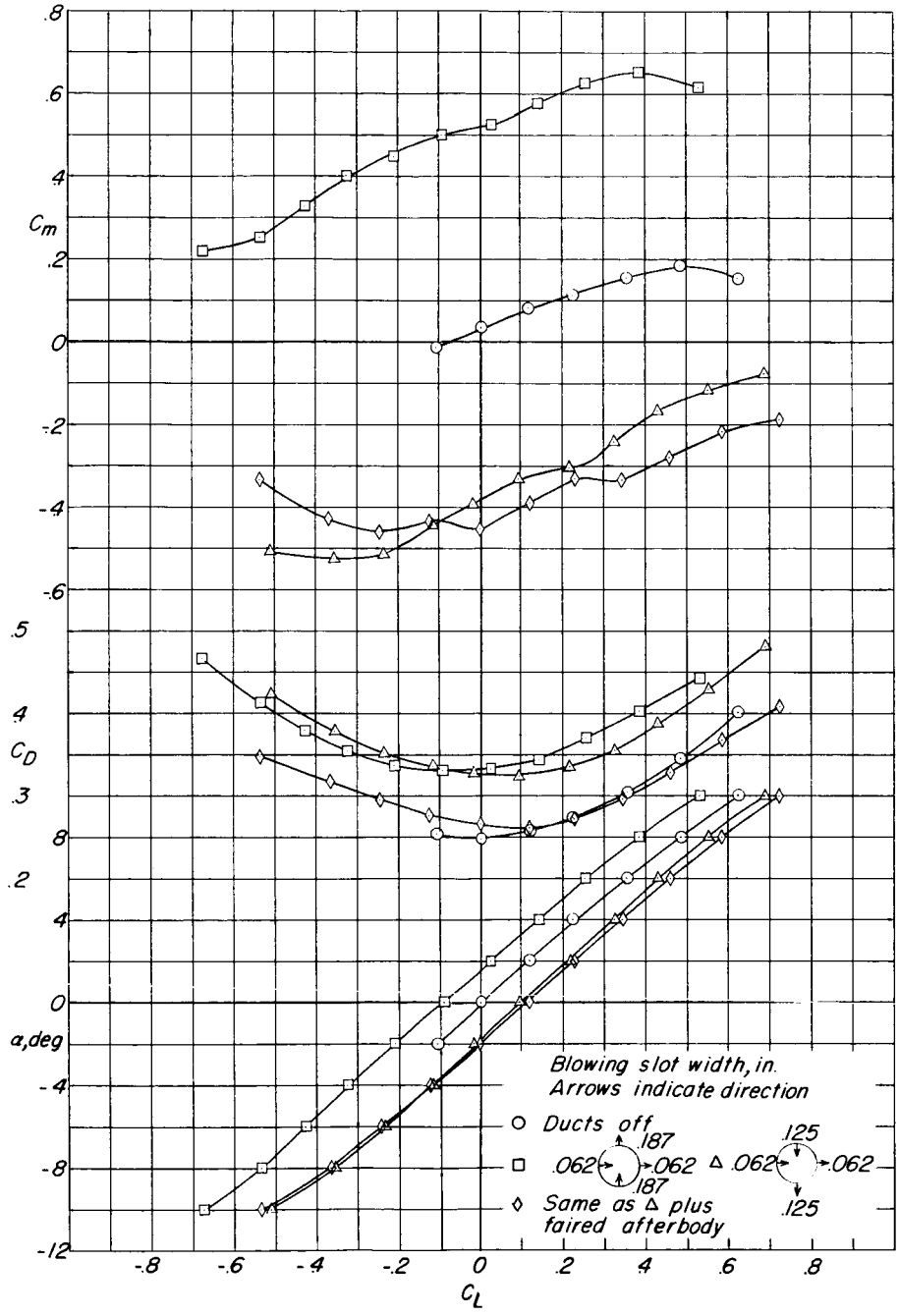

(a) M = 0.75.

Figure 15.- Effect of jet controls on aerodynamic characteristics of model 3 with and without faired afterbody. Small (0.38-inch) inside ducts. Guide feet rearward and antennas to rear of afterbody.

L-622

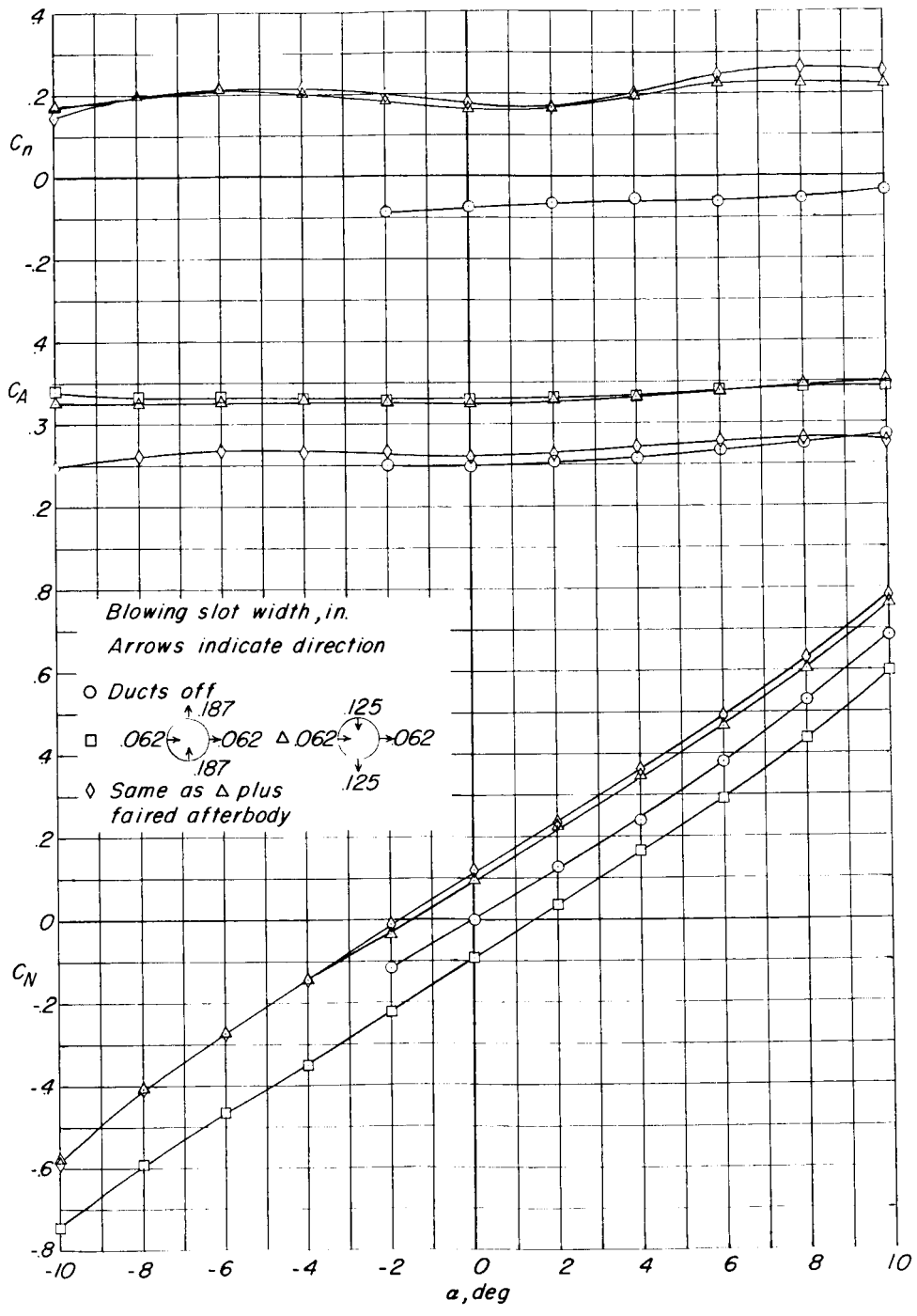

(a) M = 0.75. Concluded.

Figure 15.- Continued.

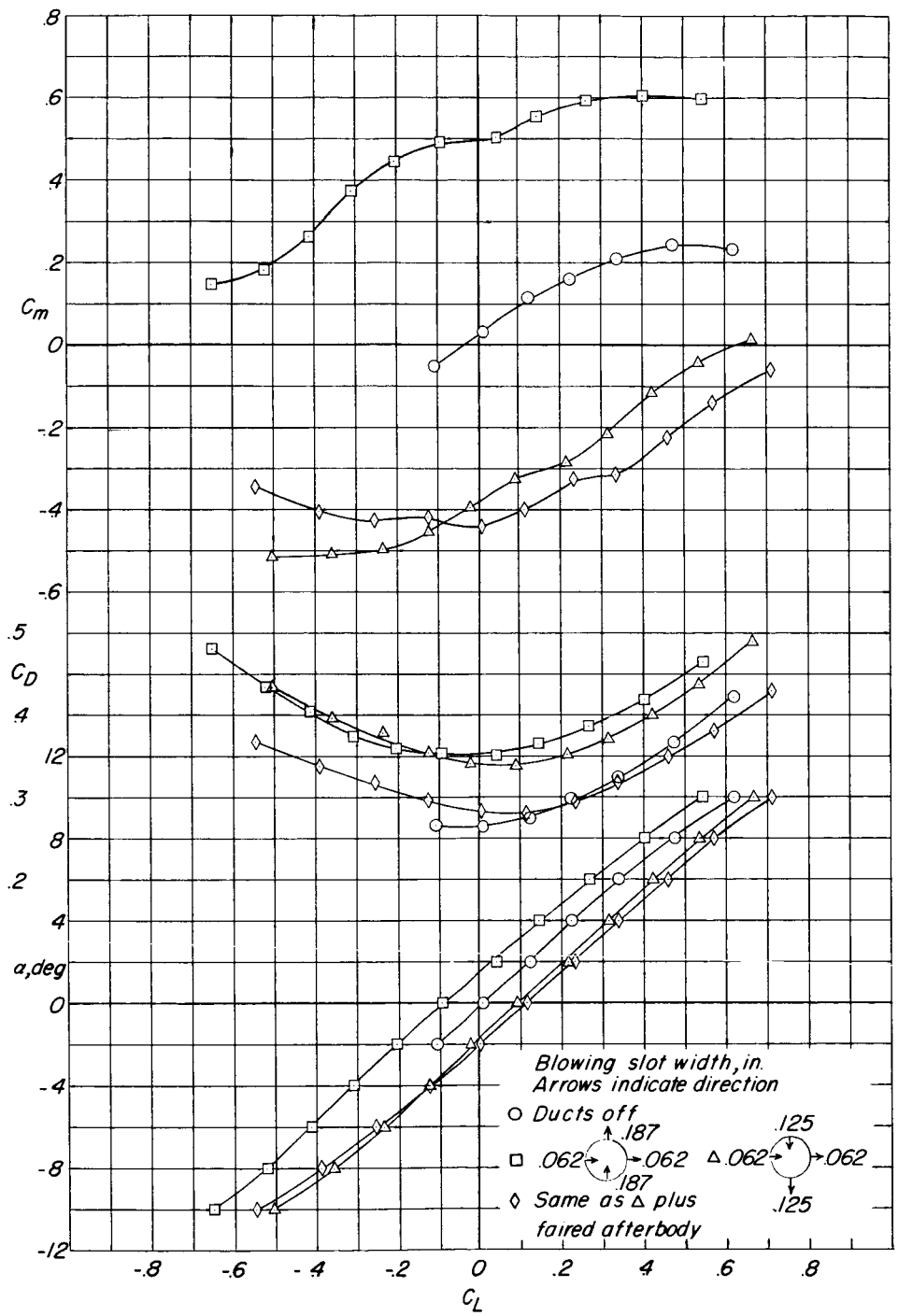

(b) M = 0.85.

Figure 15.- Continued.

[redacted]

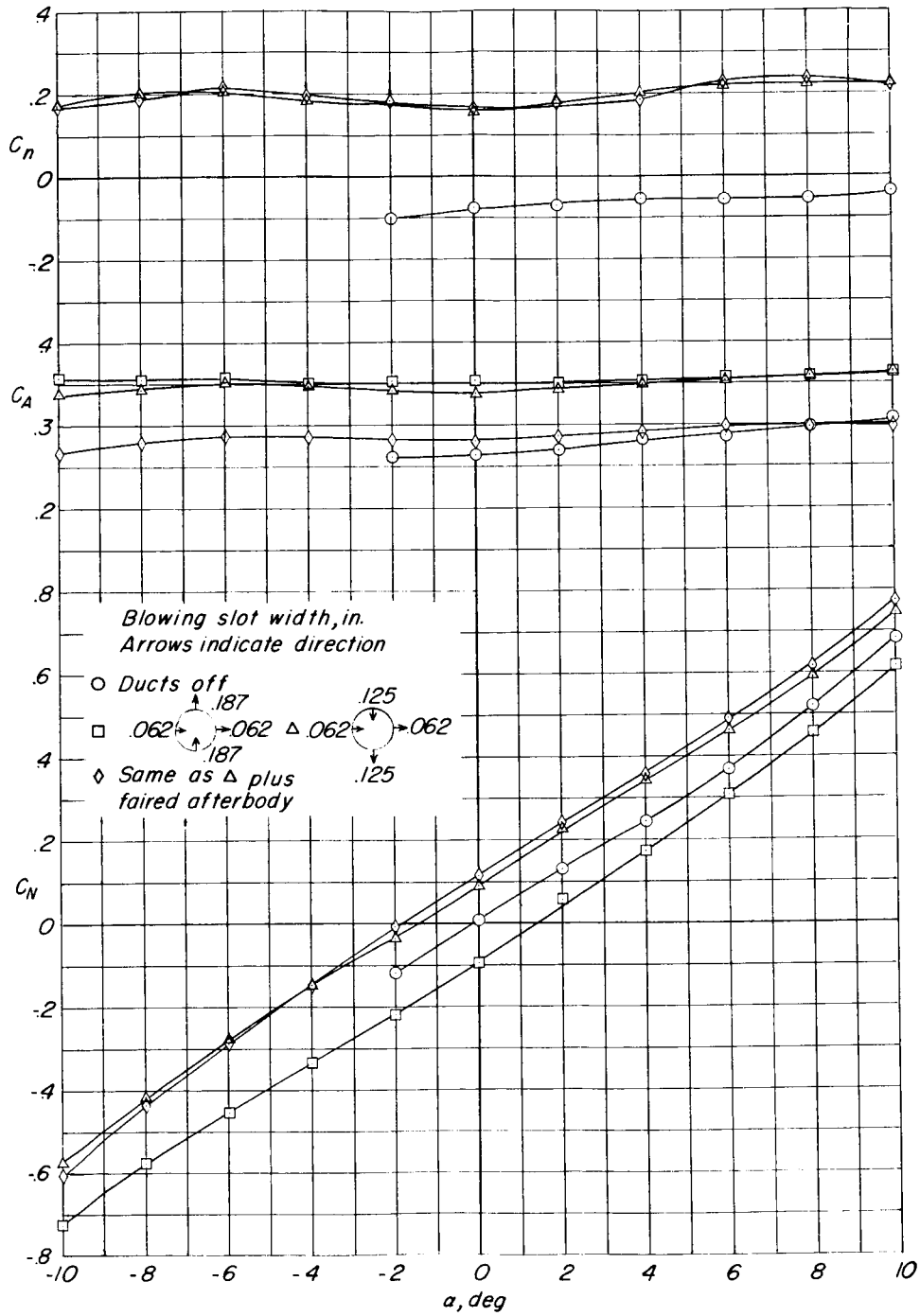

(b) M = 0.85. Concluded.

Figure 15.- Continued.

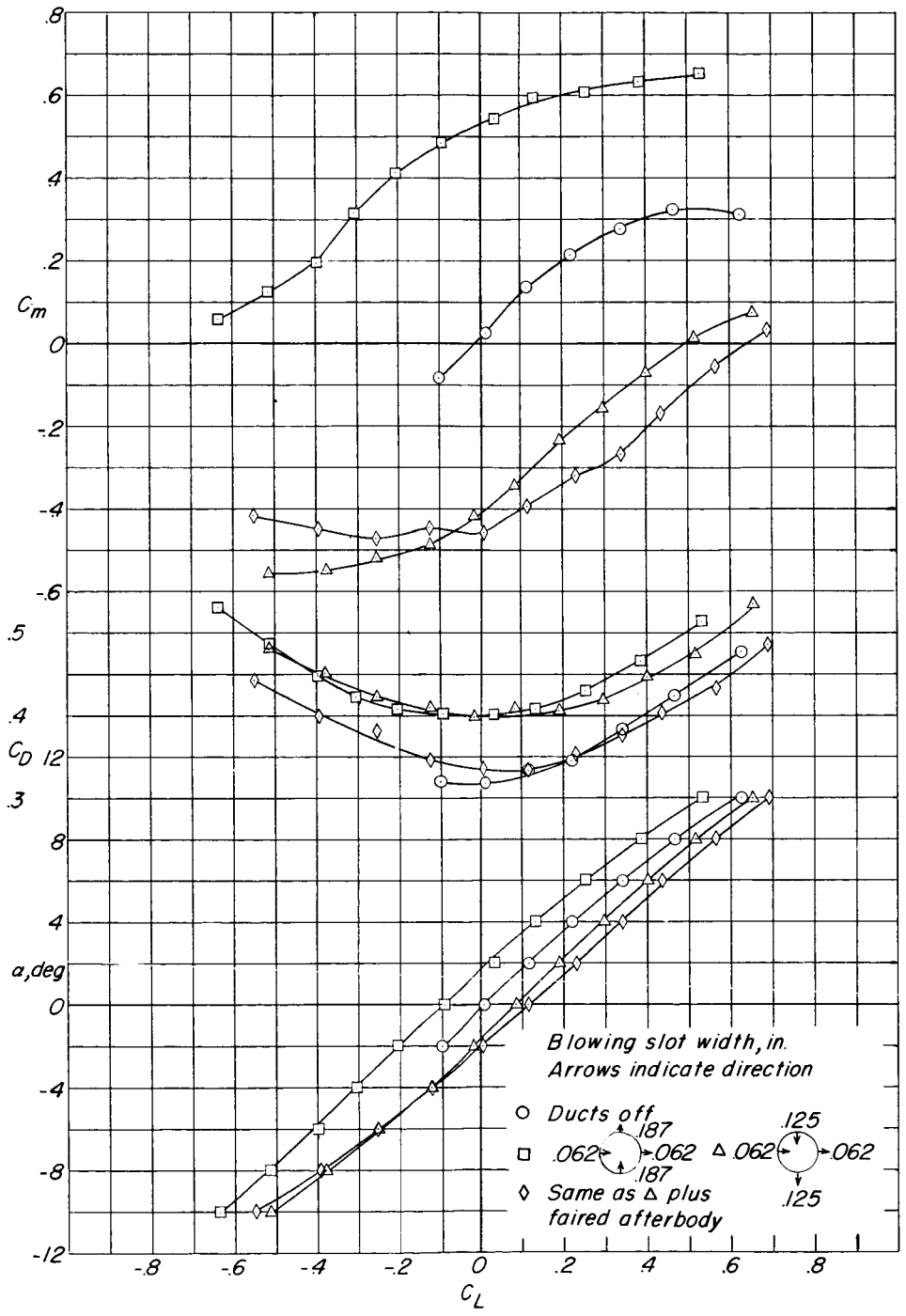

(c) M = 0.90.

Figure 15.- Continued.

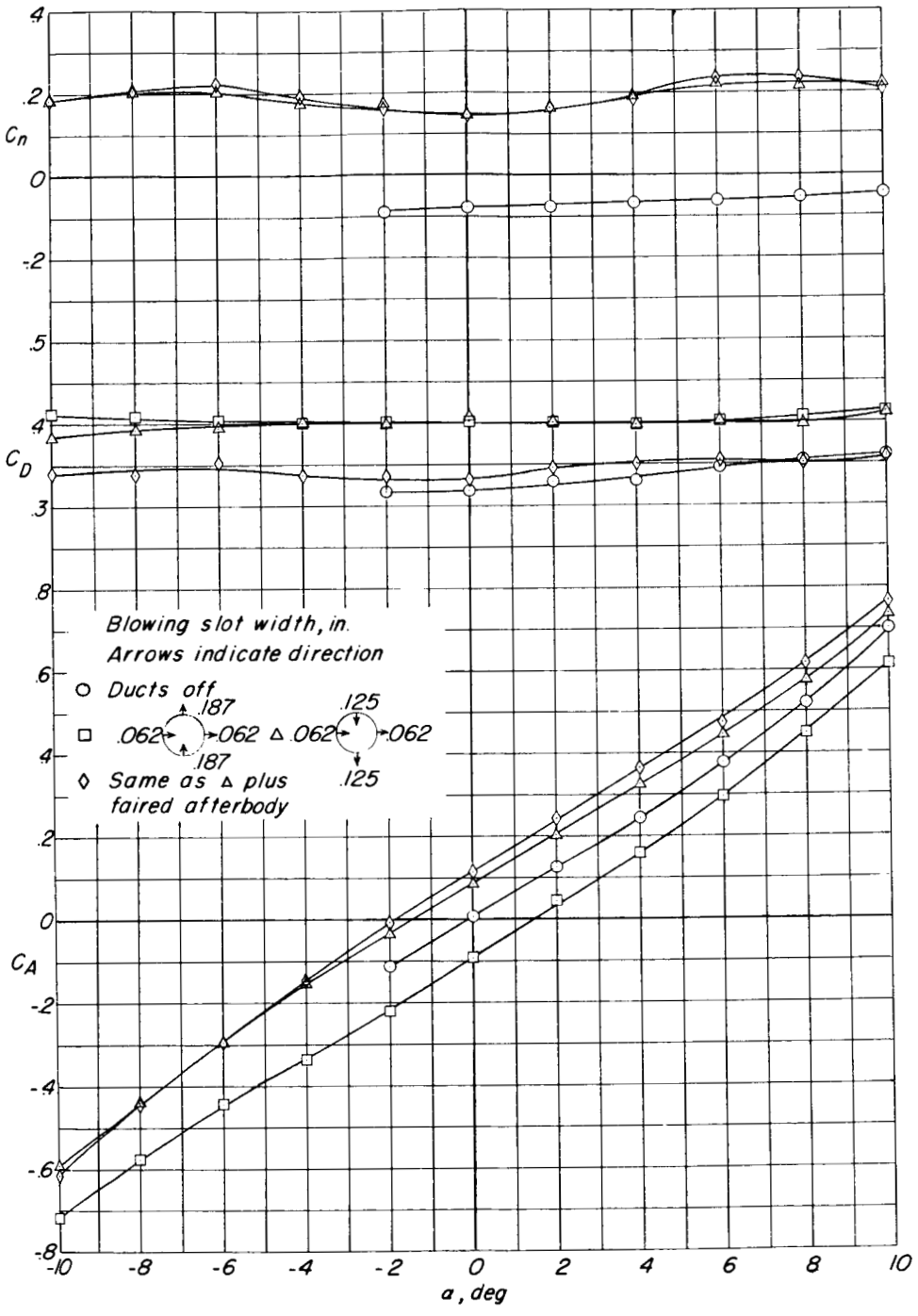

(c) M = 0.90. Concluded.

Figure 15.- Concluded.

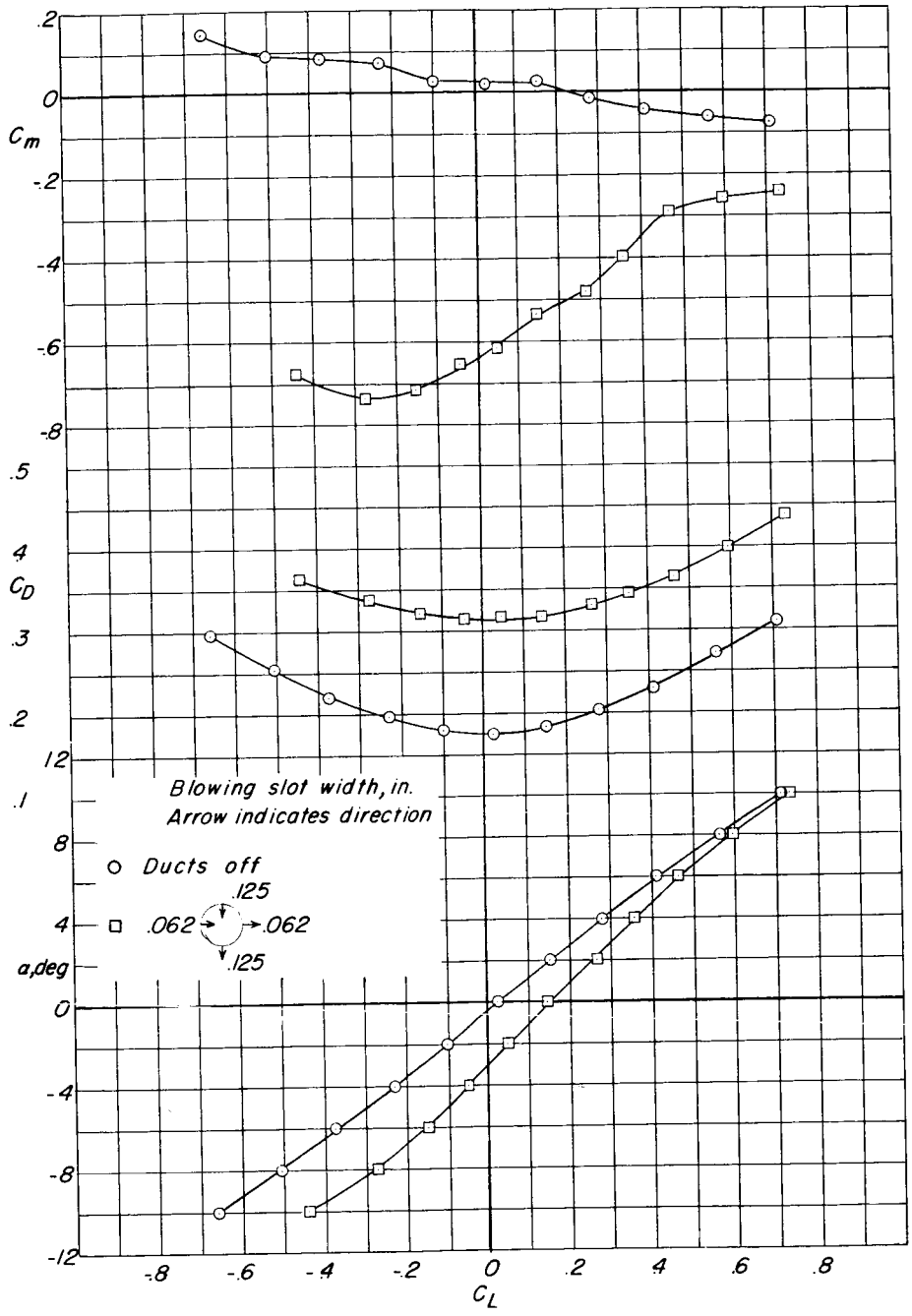

(a) M = 0.75.

Figure 16.- Aerodynamic characteristics in pitch of model 3 with jet controls. Ring tail moved rearward 0.6 inch, large (0.75-inch) inside ducts. Guide feet rearward and antennas to rear of afterbody.

L-622

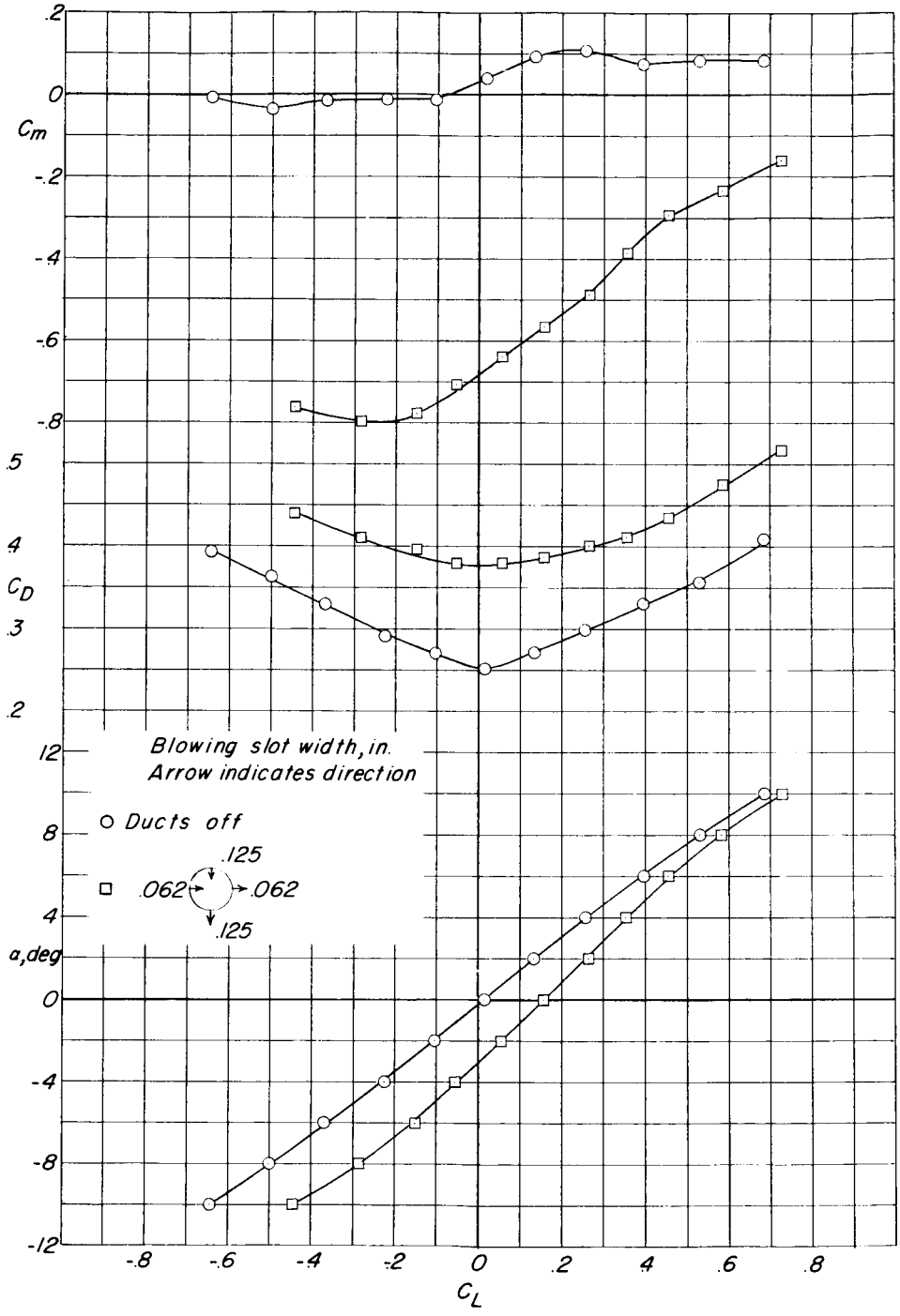

(b) M = 0.90.

Figure 16.- Concluded.

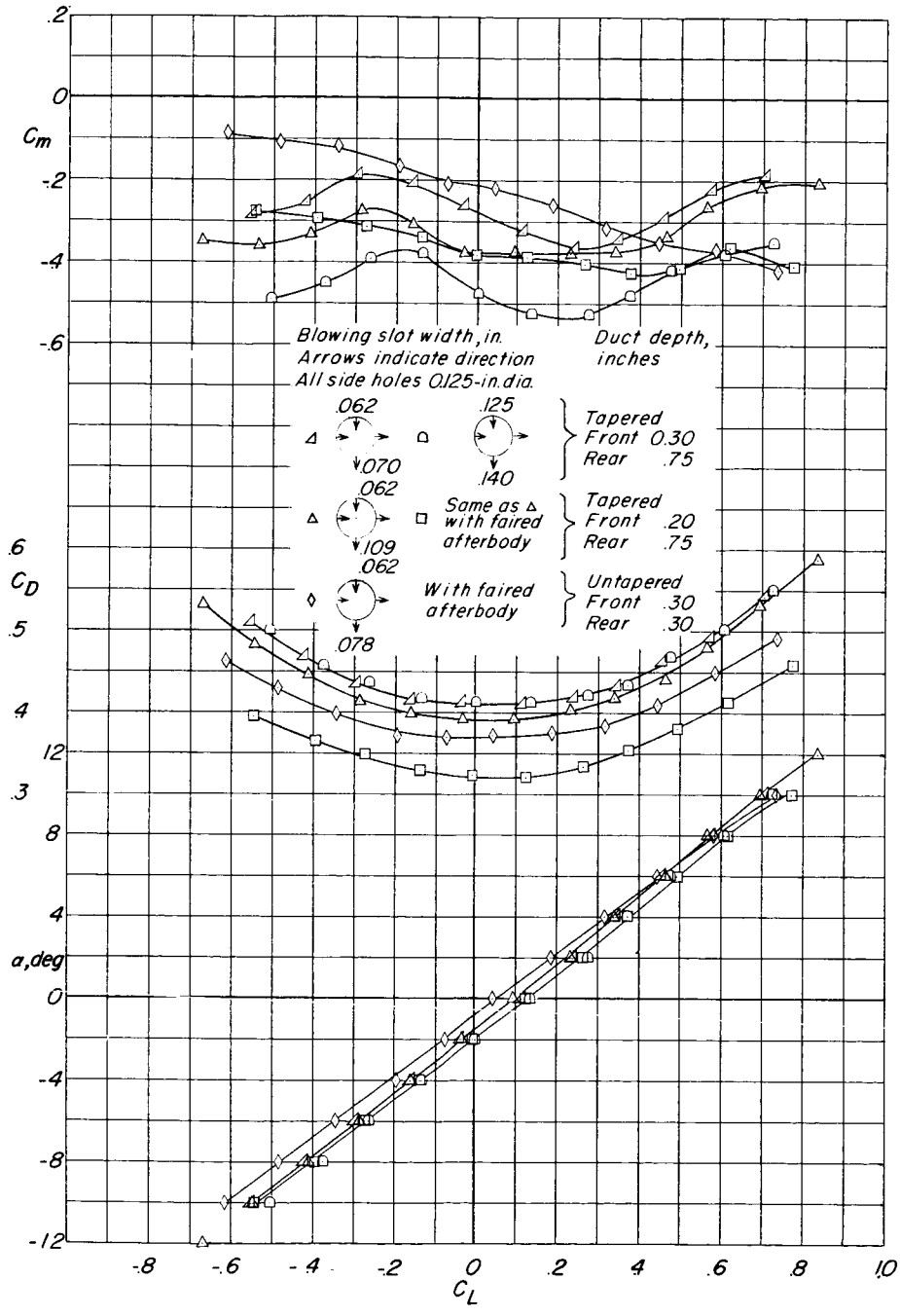

(a) M = 0.75.

Figure 17.- Aerodynamic characteristics of model 3 with jet controls and various shaped outside ducts, with and without faired afterbody. Guide feet rearward and antennas to rear of afterbody.

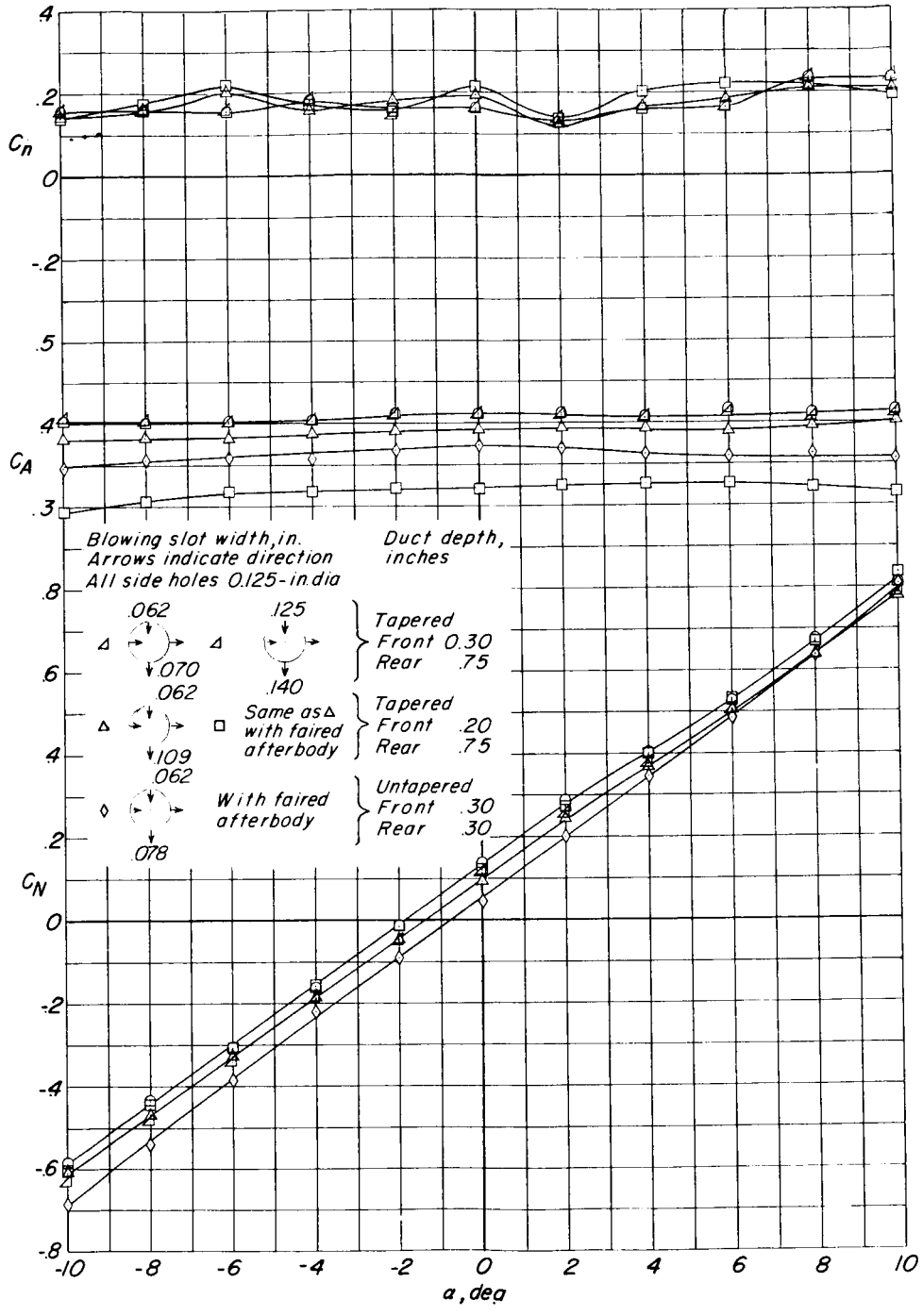

(a) M = 0.75. Concluded.

Figure 17.- Continued.

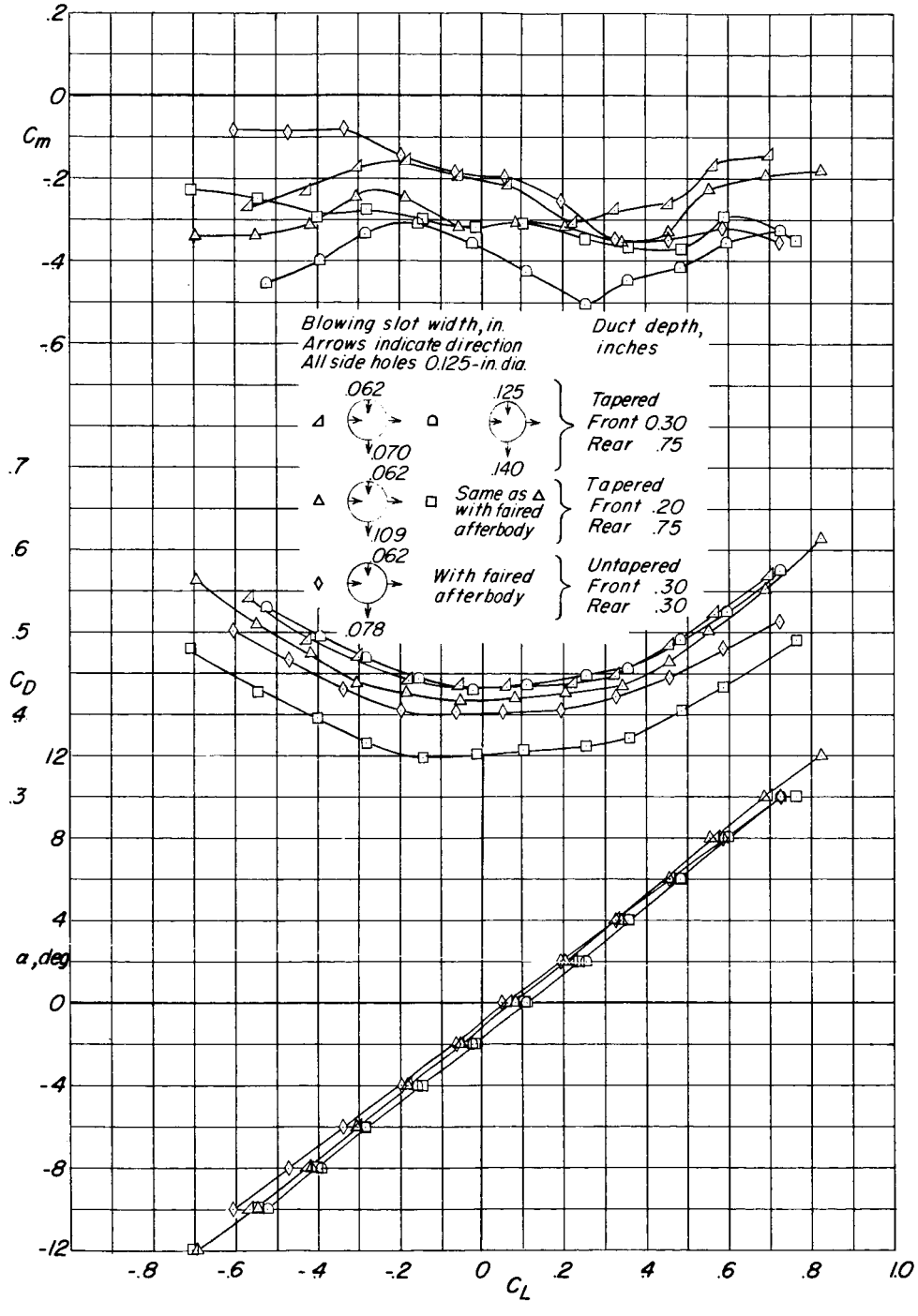

(b) M = 0.85.

Figure 17.- Continued.

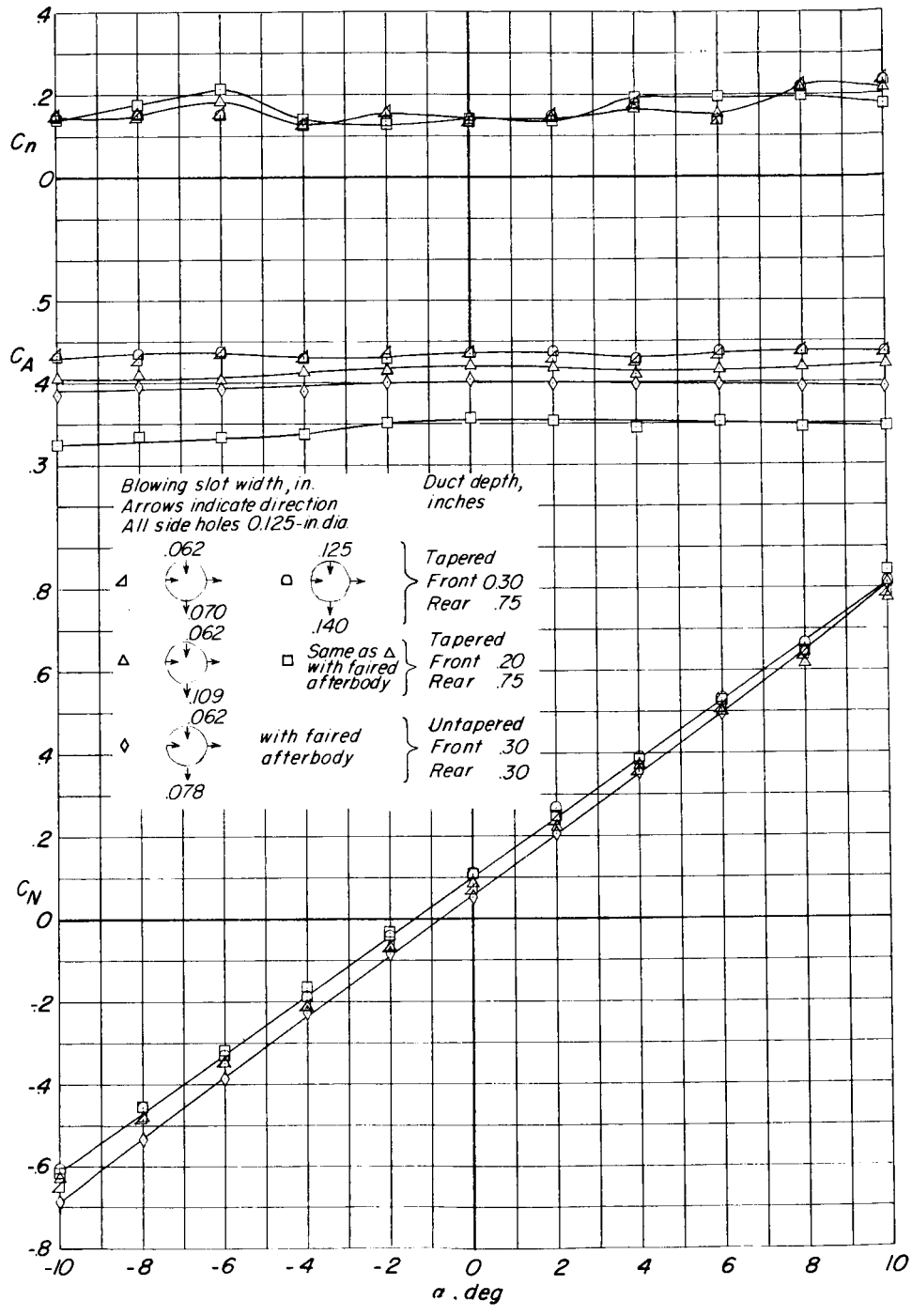

(b) M = 0.85. Concluded.

Figure 17.- Continued.

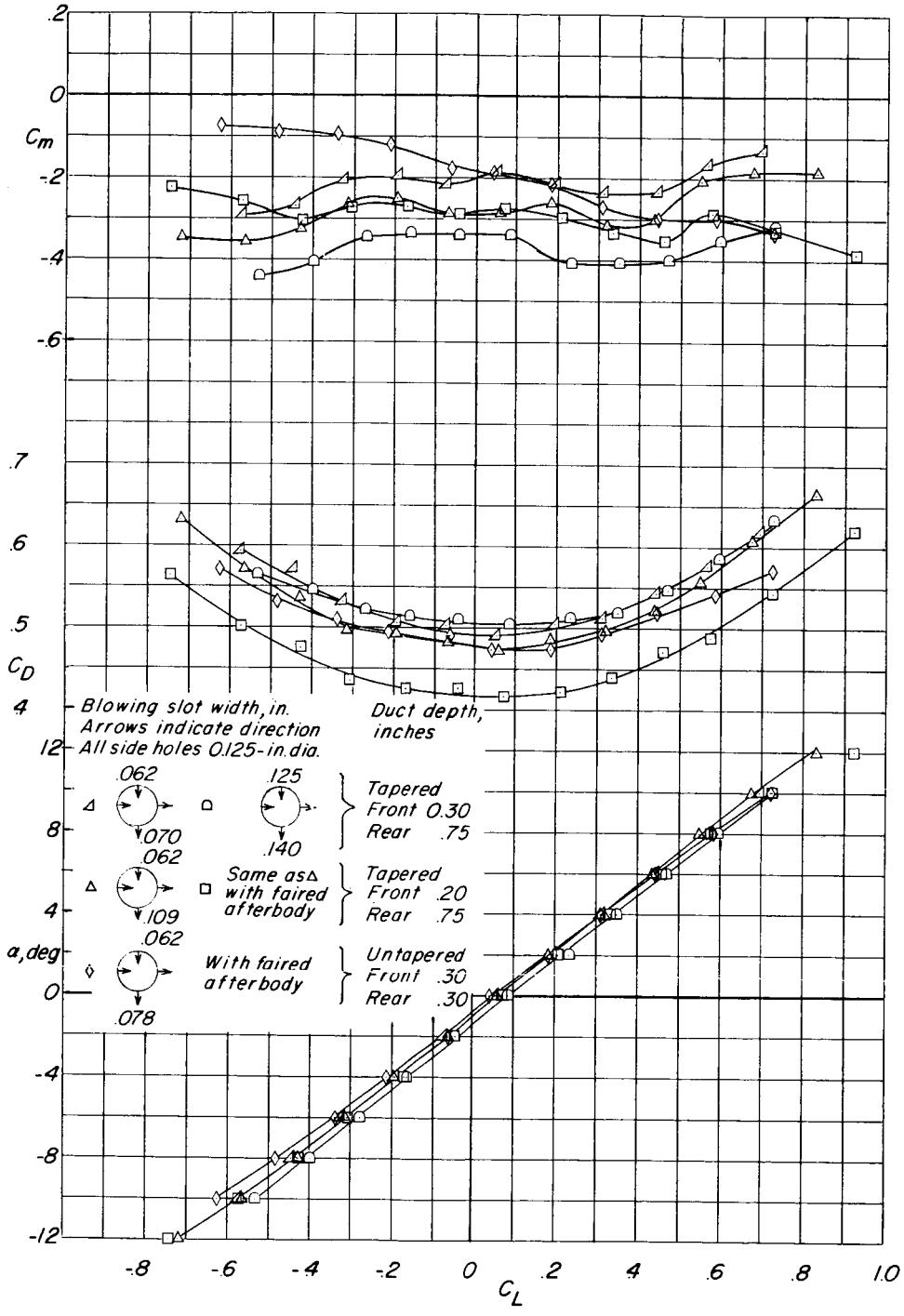

(c) M = 0.90.

Figure 17.- Continued.

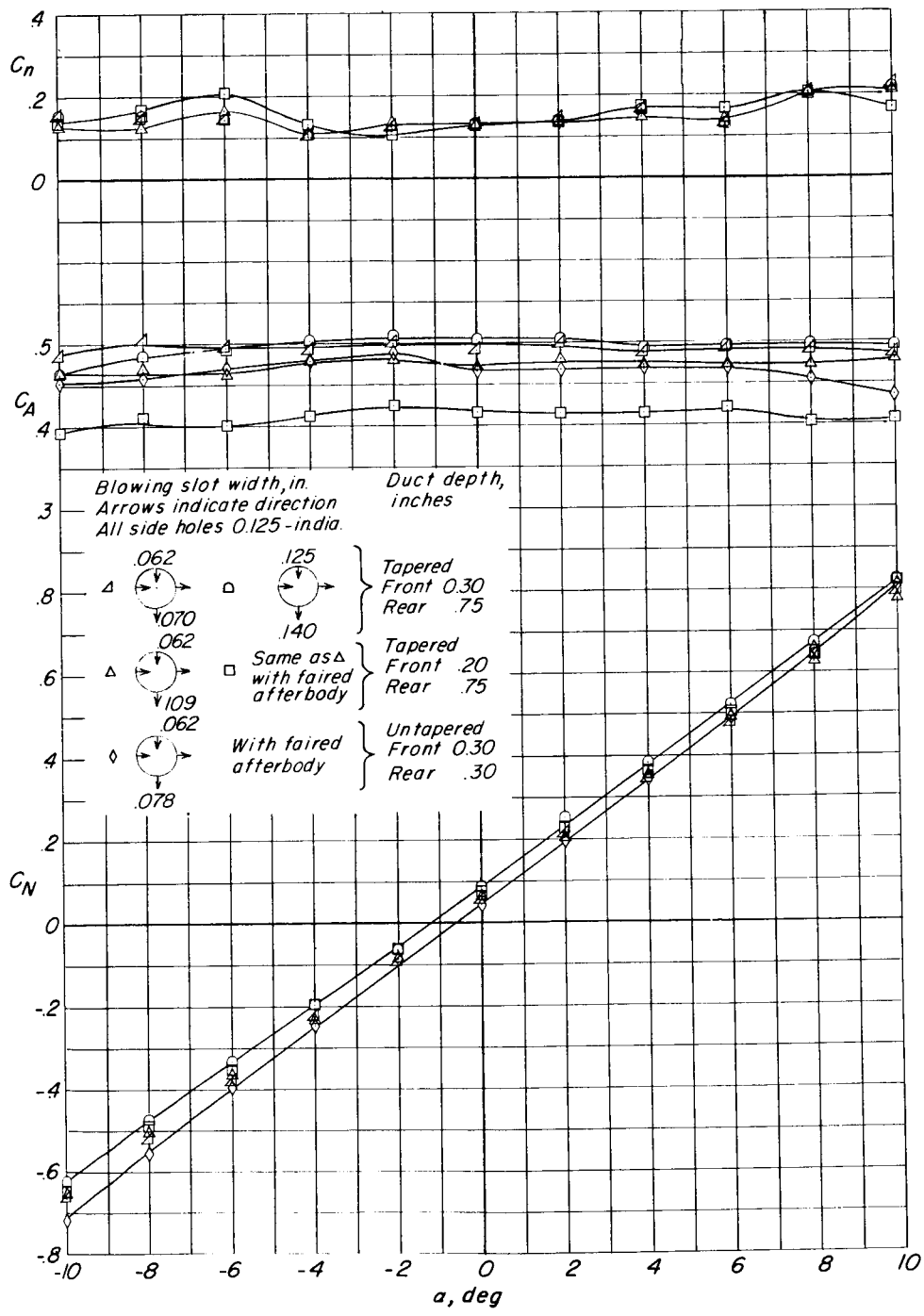

(c) M = 0.90. Concluded.

Figure 17.- Concluded.

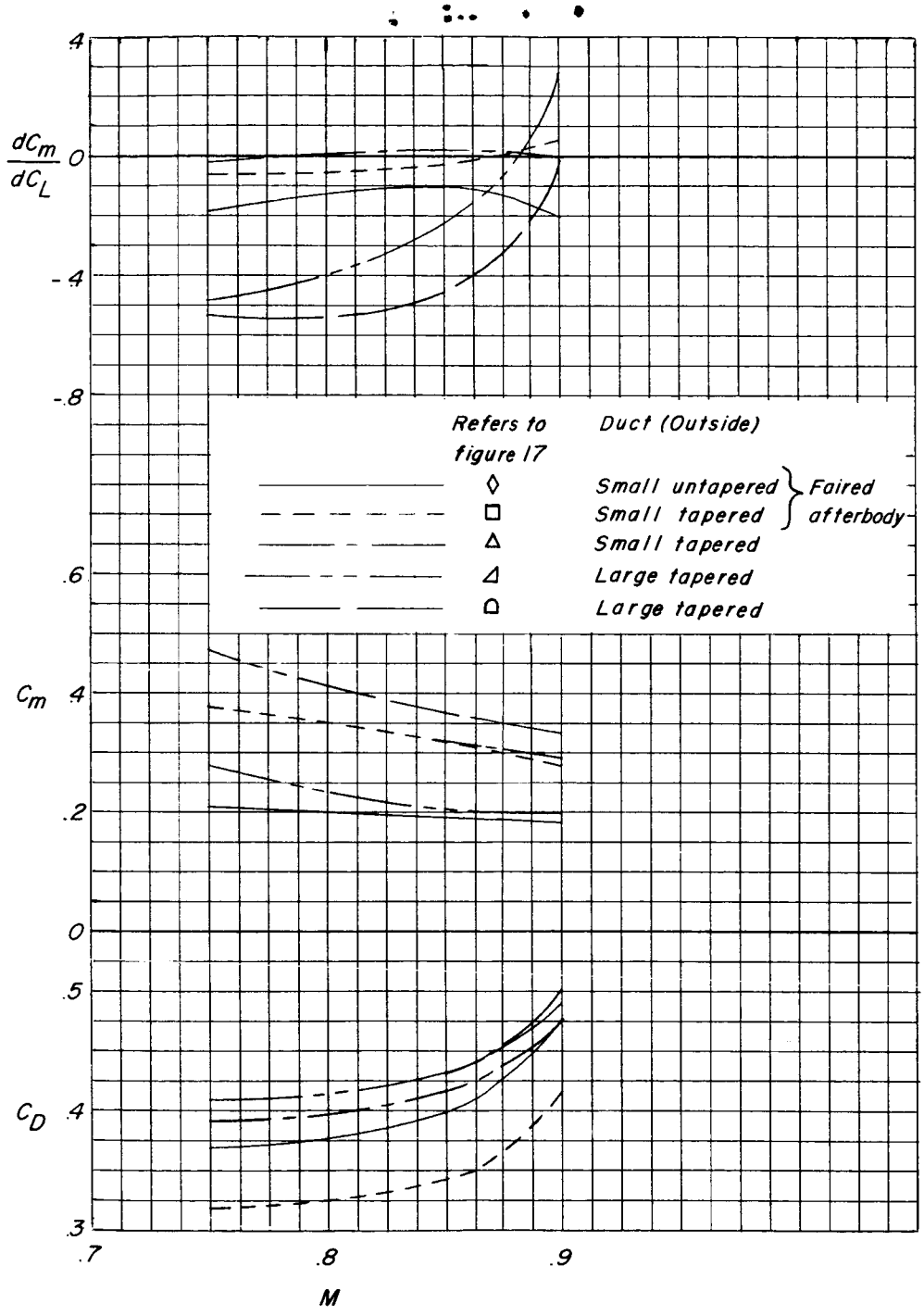

Figure 18.- Summary of the effects of duct size and shape, slot width, and afterbody fairing on aerodynamic characteristics of model 3. $\alpha = 0^{\circ}$; guide feet on.